

Estimation of the potential energy gain using salinity gradient principle in artificial saline wetlands

NISHITA GAJENDRAGADKAR

July 2022

SUPERVISORS:

Dr. IR. C. van der Tol

Dr. ING. M.J.M. Penning de Vries

ELECTRICITY FROM ARTIFICIAL SALINE WETLAND

NISHITA GAJENDRAGADKAR

Enschede, The Netherlands, July 2022

Thesis submitted to the Faculty of Geo-Information Science and Earth Observation of the University of Twente in partial fulfilment of the requirements for the degree of Master of Science in Geo-information Science and Earth Observation.

Specialization: Water Resources and Environmental management

SUPERVISORS:

Dr. IR. C. van der Tol

Dr. ING. M.J.M. Penning de Vries

THESIS ASSESSMENT BOARD:

Dr. IR. S. Salama (Chair)

Dr. Vignesh Sridharan (External Examiner, Imperial College London)



DISCLAIMER

This document describes work undertaken as part of a programme of study at the Faculty of Geo-Information Science and Earth Observation at the University of Twente. All views and opinions expressed therein remain the sole responsibility of the author and do not necessarily represent those of the Faculty.

ABSTRACT

The current global energy generation in the world is mainly reliant on fossil fuels which contribute to emission of greenhouse gases. Considering the climate change scenario, and increasing energy demands, the current energy sources should be replaced with renewable and clean energy. Salinity gradient energy (SGE) is a clean and renewable source of energy obtained when two solutions with different salinities mix. Places where naturally occurring salinity gradients exist are river mouths where river meets the sea. However, considering the importance of river as freshwater source it is essential to consider exploitation SGE using other methods. In this study, the potential of SGE is studied for theoretical artificial saline wetlands in Africa by pumping seawater to create brine in evaporation ponds. SGE can then be harnessed from the salinity gradient between seawater and the highly saline pond. The aim of the study was to estimate the energy using satellite data for different variables. The water and salt balance approach are used to determine the salinity in the evaporation ponds. In this study, suitable locations for development of an evaporation pond are identified and theoretical energy estimations are made based on different combinations for the inflow and outflow of the saline water from the pond. Furthermore, the maximum potential energy from each pond is calculated.

Keywords: Salinity gradient energy, renewable energy, evaporation pond

ACKNOWLEDGEMENTS

First and foremost, I would like to thank my supervisors Dr. IR. C. van der Tol and Dr. ING. M.J.M. Penning de Vries, for their guidance and support throughout this research. Their patience and motivation helped me to complete this research. I would also like to thank my chair Dr. IR. S. Salama for his detailed feedback during my proposal and midterm which helped me to realize and consider some important aspects for this work. Special mention to Dr. IR. W.M.de Vos for showing the membrane technology associated with this research at the laboratory in University of Twente.

I would like to thank Nilay for his constant support and faith in me even when I was doubtful about my work. I would also like to thank my friends Sahil and Arvind for helping me with the calculations in this study. My friends Sharvi and Shruti, thank you for making this journey fun and participating in all my small achievements. Last but not the least, my mother and sister for believing in me and always motivating me on my bad days. I am forever grateful for your love and support.

Table of Contents

1.	INTRODUCTION.....	8
1.1	Background.....	8
1.2	Research problem.....	9
1.3	Research objectives.....	9
1.4	Research questions.....	9
2.	LITERATURE REVIEW.....	11
2.1	Methods to harvest SGE.....	11
2.2	SGE potential estimation studies.....	13
3.	METHODOLOGY.....	15
3.1	Theoretical potential energy.....	16
3.1.1	Water balance and salt balance.....	16
3.2	Study area.....	18
3.3	Data description and preparation.....	18
3.3.1	Raster Data.....	18
3.3.2	Vector data.....	19
3.4	Site suitability.....	20
3.4.1	RET -P and coastal proximity.....	20
3.4.2	Elevation, slope and landcover.....	21
3.5	Estimation of SGE potential.....	22
3.6	Uncertainty propagation for potential SGE.....	23
4.	RESULTS.....	24
4.1	Site suitability.....	24
4.2	Theoretical SGE energy potential.....	26
4.2.1	Potential SGE and salinity of pond.....	28
4.2.2	Potential SGE and area of pond.....	28
4.2.3	Potential SGE and Q_{in} , Q_{out}	29
5.	DISCUSSION.....	30
5.1	Site specific SGE potential.....	30
5.2	Comparison with other renewable energies.....	31
5.2.1	Solar energy.....	31
5.2.2	Wind energy.....	31
5.3	Advantages and limitations of SGE in evaporation ponds.....	32
6.	CONCLUSION.....	33
7.	RECOMMENDATIONS.....	34
8.	ETHICAL CONSIDERATIONS, RISKS AND CONTINGENCIES.....	34
9.	REFERENCES.....	35

List of Figures

Figure 1 Schematic diagram of RED process (Logan & Elimelech, 2012)	11
Figure 2: Schematic diagram of the RED process (Logan & Elimelech, 2012)	12
Figure 3 Location of the RED plant on Afsluitdijk in Netherlands; Inset 3B- Schematic of the RED plant operation	12
Figure 4 Overall methodology flowchart.....	15
Figure 5: Conceptual diagram for the water balance in the evaporation pond.....	17
Figure 6: (A) RET-P map with the locations of 5 sites (B) Site 1 showing the 100 km coastal proximity	21
Figure 7: Landcover classification- site 1	22
Figure 8: Site 1 suitability map	24
Figure 9: Site 2 suitability map.....	25
Figure 10 Site 4 suitability map.....	25
Figure 11 Site 3 and 5 suitability maps	26
Figure 12: Q_{in} factor vs salinity of largest pond at every site.....	28
Figure 13: Q_{in} and Q_{out} vs. potential SGE for area of 1307 km ² in site 1.....	29
Figure 14: Q_{in} and Q_{out} vs. potential SGE for area of 283 km ² in site 2.....	30
Figure 15: Q_{in} and Q_{out} vs. potential SGE for area of 217 km ² in site 4	30
Figure 16 Total precipitation (mm) Africa -2019	40
Figure 17 Total Reference evapotranspiration in Africa(mm)-2019.....	40
Figure 18 : Q_{in} and Q_{out} vs. potential SGE for area of 108 km ² in site 1	Error! Bookmark not defined.
Figure 19 : Q_{in} and Q_{out} vs. potential SGE for area of 217 km ² in site 1	41
Figure 20 : Q_{in} and Q_{out} vs. potential SGE for area of 434 km ² in site 1	42
Figure 21 : Q_{in} and Q_{out} vs. potential SGE for area of 219 km ² in site 2	Error! Bookmark not defined.

List of tables

Table 1: Estimations of potential SGE from different studies.....	13
Table 2: Summary of the datasets used in the study	Error! Bookmark not defined.
Table 3: Elevation and slope for the five sites	21
Table 4 Area size of ponds at the 5 sites.....	23
Table 5: Theoretical SGE potential for each pond	27
Table 6: Relationship between area change and energy gain	29

1. INTRODUCTION

1.1 Background

The current global energy generation is mainly reliant on the combustion of fossil fuels which is one of the major contributors to greenhouse gas (GHG) emissions and ultimately to climate change (Arias et al., 2019). The urgent need to combat climate change as well as fulfill the rising energy demands needs a global energy transformation which is reliant on low-carbon power. Moreover, the supply of fossil fuels is limited giving us the opportunity to shift to renewable sources of energy which will alleviate the adverse environmental impacts (Marin-Coria et al., 2021; Mendoza et al., 2019). Increasing access to renewable energy is the most promising way to eliminate the use of fossil fuels (Olabi & Abdelkareem, 2022). The search for alternative and sustainable energy sources is one of challenges we face today as the source should be environmentally friendly, freely available, reliable, and renewable.

The Sustainable Development Goal (SDG) 7 aims to “Ensure access to affordable, reliable, sustainable, and modern energy for all”. By 2030, the SDG 7 seeks to increase the share of renewable energy in the global energy mix as well as boost access to clean energy (*Goal 7 | Department of Economic and Social Affairs, 2022*). Wind power, hydropower, biomass, geothermal energy, solar energy are renewable, sustainable, and clean sources of energy. Together with these energy sources, the Marine Renewable Energies (MREs) or ocean energy are being explored to harness the enormous energy from the natural activities occurring in the marine environment (Castelos, 2014; Goffetti et al., 2018). The sources of MREs are tidal range and currents, waves, ocean currents, ocean thermal energy conversion and salinity gradients (Lewis et al., 2011). Although any substantial progress in technologies to harness MREs is unlikely to occur before 2030 (Castelos, 2014), the theoretical potential for MREs is immense and projected at 7.4×10^{21} J/year (Lewis et al., 2011). The use of MREs can fulfil majority of the energy demands as they provide energy through decentralized grids to the coastal regions which are focal points of intense urban, trade, and industrial activities (Zachopoulos et al., 2022).

Amongst all the sources of ocean energies, the salinity gradient energy (SGE), also called osmotic power or blue energy (Yin Yip et al., 2016) is contained within a system when two aqueous solutions having different salt concentrations mix. The mixing releases free energy which arises due to the difference in chemical potential between the two solutions and can be used to produce power (Emdadi et al., 2016; R. Pattle, 1954; Reyes-Mendoza et al., 2020). In nature, the locations where rivers (low salinity) meet oceans or hypersaline lakes (high salinity) are the potential areas for harnessing SGE (Jia et al., 2014a). The global theoretical SGE potential based on the discharge of all rivers in the ocean is estimated between 1.4 to 2.6 TW (Emdadi et al., 2016) which may satisfy 40% to 80% of the global electricity requirements (Kuleszo et al., 2010). The theoretical SGE per continent based on the annual continental discharge data was estimated by (Stenzel & Wagner, 2010) in which they concluded Asia as the continent with highest potential. Furthermore, SGE has nearly zero GHG emissions and minor environmental impact (Emdadi et al., 2016; Jia et al., 2014b). These estimations exclude other systems like brine water from desalination units which can also be used to produce SGE. Thus, the importance of this process on the global level cannot be underestimated, especially when we are in dire need of alternative and clean energy sources.

Practically, only a small portion of the theoretical potential energy can be utilized. Factors like pumping power in transportation of sea and river water to power plant, the amount of usable river water and variability in the seasonal discharges of different rivers reduce the amount of SGE that can be harvested (Stenzel & Wagner, 2010). Moreover, many of the freshwater systems feeding human populations are stressed and as a result, globally about 1.1 billion people lack access to freshwater (*Water Scarcity | Threats | WWF, 2022*). Rivers are major and valuable sources of freshwater and their use for SGE generation may not be compatible with other uses of freshwater, including drinking water, in water scarce areas.

A new approach to harness SGE by storing saline water in ponds in flatland locations remains unexplored (Kempener & Neumann, 2014). The idea of such saline ponds or evaporation ponds along the coast was mentioned by Gerald Wick (Wick, 1978). In this case, the salinities higher than Dead Sea can be maintained by monitoring influx of seawater. The salinity gradient then would be created between the brine in saline pond and seawater. Helfer and Lemckert proposed the idea of pumping seawater in lakes and decreasing the volume of lake due to evaporation, subsequently increasing the salinity of lake (Helfer & Lemckert, 2015). Energy can then be harvested from the salinity difference between sea and concentrated lake water. The authors proposed Lake Torrens and Lake Eyre located in South Australia as feasible locations for saline ponds as they remain dry almost throughout the year due to high annual evaporation and low rainfall. Such a combination of seawater and brine water is advantageous as it does not use freshwater from rivers which are major and valuable freshwater resources. With this approach, renewable energy can be harnessed without being a threat to freshwater resources. Moreover, this approach is beneficial as it is not constricted by the temporal variability of the river flows.

In the past few years Africa has seen great global population and economic growth. However, scarcity of clean water and lack of proper electrification are some of the major challenges African countries face as almost 62% of population is without access to electricity (De Angelis et al., 2021). To satisfy the growing energy demands while considering the climate change scenario, renewable energy will have an important role, opening new opportunities for innovation and growth in the African energy sector. Generation of SGE by using saline ponds will produce clean and renewable energy but not at the expense of freshwater which is already in short supply for most of the countries on this continent. Moreover, Africa has a long coastline, year-round solar radiation and high evaporation rates which can be used as an advantage for the development of saline ponds to harvest SGE. This theoretical study is carried out to estimate the potential SGE using hypothetical artificial saline pond at some selected sites in Africa.

1.2 Research problem

The SGE potentials from the studies so far were estimated using data from *in situ* measurements, literature review or from laboratory experiments (see section 2). Furthermore, the saline ponds using seawater as the dilute solution to harness SGE has not been studied by many authors. The use of satellite data to assess the SGE potential has not yet been implemented in any of the previous works. The in-situ networks that provide data on sea surface salinity, precipitation or other variables are scarce in many parts of the world. Remote sensing provides expanded spatial coverage, high measurement frequency and lessened risk to people going on fields in rough terrains. Remote areas or areas which are inaccessible to carry out the field measurements can be covered by remote sensing. Moreover, availability of near real time data is beneficial to address the study in the current conditions. This research focuses on using the water balance approach using remotely sensed datasets to calculate the theoretical potential SGE in an artificial wetland.

1.3 Research objectives

The main objective of this study is to use **satellite data** to **estimate the maximum potential energy gain** using salinity gradient principle in artificial saline wetlands.

Sub- objective 1: To identify a suitable area for an artificial wetland for SGE generation in Africa

Sub-objective 2: To estimate the maximum potential energy gain using water and salt balance equations

1.4 Research questions

Sub-objective 1:

Research question 1: What are the relevant variables to be considered for identifying suitable area for evaporation pond?

Research question 2: Where are the suitable areas for energy generation located?

Sub-objective 2:

Research question 1: Which combination of parameters is most suitable for energy generation in the artificial wetland?

Research question 2: What is the maximum potential energy gain from the artificial wetland?

2. LITERATURE REVIEW

2.1 Methods to harvest SGE

When two solutions with different salinities mix free energy is released which can be lost as heat if the mixing is uncontrolled (Yin Yip et al., 2016). To harvest SGE, controlled mixing of the two solutions is required which can be achieved by different processes. Although many techniques have been described to harvest SGE, Pressure retarded osmosis (PRO) and reverse electrodialysis (RED) remain the most studied technologies (Budi et al., 2021; Haddout & Priya, 2020; Sharma et al., 2022). Thus, this section will give a brief overview of these two processes.

The PRO method was first described by Prof. Sidney Loeb in 1975 (Loeb & Norman, 1975) and has undergone improvements over the years. In this method, the dilute solution, known as the feed, is separated from a pressurized and concentrated (saltier) solution by a semipermeable membrane which allows the passage of water, but no ions. The concentrated solution (draw) solution pulls the feed solution through the membrane. This dilutes the draw solution increasing the volume flow rate of water and the resulting high pressure solution is used to run the turbine to produce power (Helfer et al., 2014; Logan & Elimelech, 2012). Figure 1 shows a diagram of energy generation using PRO for river water vs. seawater. The Norwegian company, Statkraft established the first osmotic power plant based on PRO in 2009, however due to high operating costs, the plant was closed for further developments.

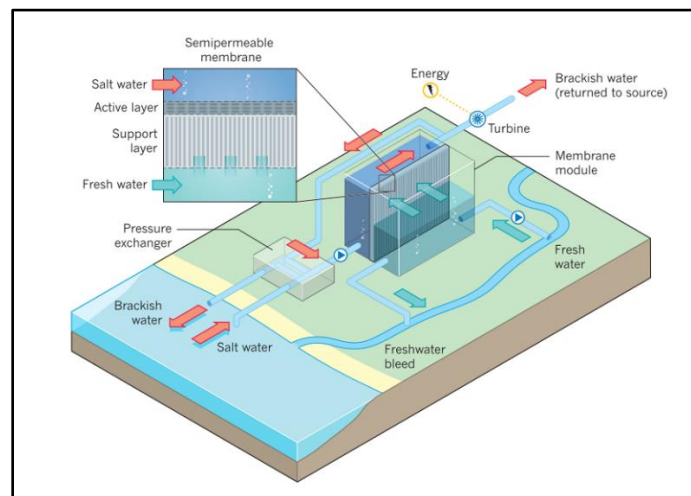


Figure 1 Schematic diagram of RED process (Logan & Elimelech, 2012)

The second approach, RED was first described by Pattle in 1954 (Pattle, 1954). It uses ion-selective membranes which allow passage of either negatively charged or positively charged ions. The stack of membranes is arranged in an alternating pattern and the sections between them are alternately filled with a concentrated salt solution and diluted salt solution. The cations and anions move in the opposite direction and the ion current formed is used to produce electrical power (Logan & Elimelech, 2012; Post et al., 2007; Veerman et al., 2010; Wick, 1978). The RED approach was studied in laboratory by an institute in Netherlands. Its spin-off company REDstack operates the first RED plant since 2014 which is located on the Afsluitdijk in the Netherlands (Schaetzle & Buisman, 2015). Figure 2 shows a schematic diagram of the RED process whereas Figure 3A and 3B show the location and schematic diagram of the RED plant operated by REDstack respectively.

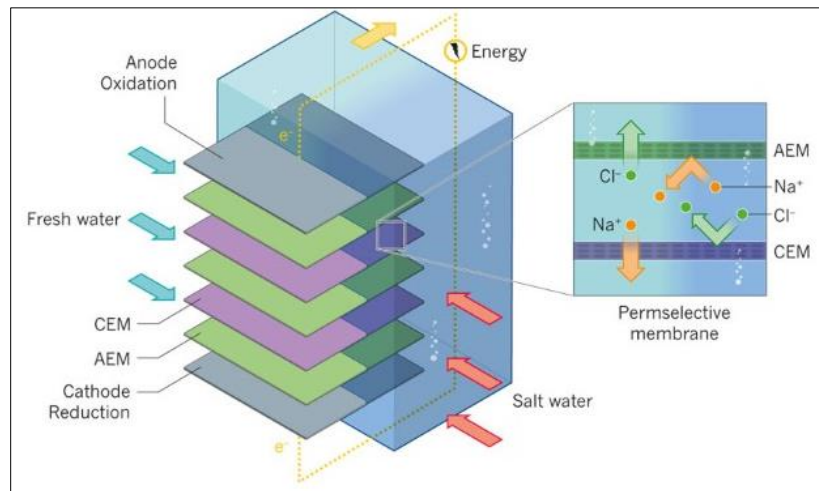


Figure 2: Schematic diagram of the RED process (Logan & Elimelech, 2012)

In Figure 2, the blue arrows indicate fresh water while the red arrows represent saltwater. The energy generated by mixing of these waters is harvested by the cation-exchange membranes (CEMs) and anion-exchange membranes (AEMs).

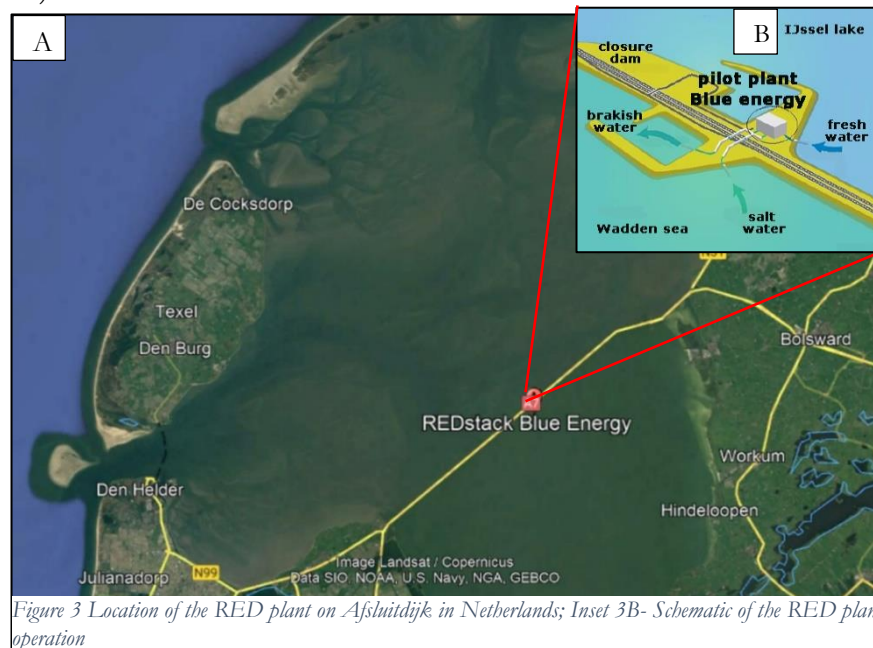


Figure 3 Location of the RED plant on Afsluiddijk in Netherlands; Inset 3B- Schematic of the RED plant operation

The main difference between PRO and RED is that PRO uses the water flux through membranes for electricity generation while RED relies on ion flux across the membranes (Logan & Elimelech, 2012). A study by (Post et al., 2007) comparing both these techniques concluded that PRO is suitable for SGE generation using concentrated saline brines while RED performs well for power generation using seawater and river water. The advantages of PRO over RED considering factors such as membrane materials and power density was described by (Sharma et al., 2022). The energy efficiency and power density performance of PRO and RED was examined by (Yip & Elimelech, 2014). This study concluded that PRO could attain better efficiencies and power densities over RED as PRO membranes restrain the harmful leakage of salts and make use of the salinity difference more efficiently. Apart from the comparative studies, numerous studies have also investigated the performance of PRO (Lin et al., 2014; Thorsen & Holt, 2009) and RED (Danilidis et al., 2014; Długolęcki et al., 2009; Vermaas et al., 2012) independently. Although both the technologies are in constant development, the technical potential for real scale plants remains unclear but may increase with the improvement of membranes and other components.

2.2 SGE potential estimation studies

Several studies have been carried out to estimate SGE potentials on global, continental, and country level. Most of the studies investigate the SGE potentials for the mixing of river water and seawater. The global SGE potential is reported to be 1650 TWh/year by (Thorsen & Holt, 2009; Yip et al., 2011) and 27 TWh/year by (Stenzel & Wagner, 2010). The latter study also calculated technical and ecological potential by considering constraints like pumping power for transporting the river and seawater and amount of usable river water. In the same study, the SGE potentials on continental level were estimated using the annual river discharge values from the Global Runoff Data Centre (GRDC) model. The theoretical and technical potential for 16 river basins in China was estimated as 0.04 TW and 0.022 TW respectively (Kuleszo et al., 2010). This study also assessed the future trends of SGE, for the years 2030 and 2050, and the possible effects on greenhouse gas emissions if coal was replaced by SGE in electricity production. The SGE potential of 10 rivers in Quebec, Canada was estimated by (Maisonneuve et al., 2015) to be 30 TWh/year. The authors also considered the variations in river flow rate, concentration and temperature and concluded that the lowest power potential was enough to meet the entire power requirements in Quebec region. Estimations of SGE potentials for particular rivers and seawater have been reported from different studies which are summarized in Table 1. Furthermore, SGE potentials have also been calculated for rivers entering hypersaline systems like Lake Urmia in Iran, Lake Eyre and Torrens in Australia are also summarized in Table 1.

Table 1: Estimations of potential SGE from different studies

Authors	Combination of aqueous solutions (Concentrated vs. dilute)	Study site
(Wick, 1978)	Seawater vs. river water	Amazon river, Brazil
(Loeb, 2002)		La Plata-Parana River, Argentina
(Helfer & Lemckert, 2015)		Congo River, Congo
(Jahromi et al., 2015)		Yangtze River, China
(Alvarez-Silva & Osorio, 2015)		Ganges River, Bangladesh
(Khodadadian Elikaiy et al., 2021)		Mississippi river, United States
(Zachopoulos et al., 2022)		Brisbane river, Australia
(Helfer et al., 2014)		Bahmanshir River, Iran
(Wick, 1978)	Brine from hypersaline systems vs. river water	Magdalena river, Colombia
(Loeb, 2001)		Arvand River, Iran
(Helfer & Lemckert, 2015)		Strymon river, Greece
(Emdadi et al., 2016)		Great Salt Lake, United States
		Dead sea, Israel
		Great Salt Lake, United States
		Lake Eyre and Lake Torren, Australia
		Lake Urmia, Iran

Even though sea water and river water make a great combination for harnessing SGE, the importance of rivers as a freshwater source limits the usage of entire river flow for this energy. Thus, search for alternative salt solutions for SGE extraction is necessary. Apart from the studies focusing on natural salinity gradients (river water vs seawater/brine water), some research has also been done on estimation of SGE potentials for brine water from industrial or desalination units. As opposed to the studies in Table 1 (Kang et al., 2022) studied the capture of SGE from desalination unit using the RED method wherein they calculated the SGE potential by using real seawater as diluted solution and seawater discharged from desalination unit as the concentrated solution. They observed that using seawater as dilute solution increases the power density but the sediments in the discharged seawater can be harmful for the membranes, however this limitation can be removed by filtration of the sediments. Five real water pairs consisting of river water, seawater, desalination brine, saline water from pickling plant and treated wastewater, collected from different sites in North Carolina, USA were examined for the effect of natural organic matter and inorganic solutes on power densities using RED method (Kingsbury et

al., 2017). The maximum power density was from pickling plant water and the river water. A coal-mine brine solution was stimulated by (Turek et al., 2008) to study the economic feasibility of SGE that could be obtained from salinity gradient produced by coal—mine brine and river water in Poland. (Zoungrana et al., 2020) estimated the SGE potential from treated wastewaters discharged in Marmara Sea in a lab-scale RED setup. Thus, river water or freshwater is not the only option which can be utilized as the diluted solution component for the recovery of SGE. Moreover, development of suitable and cost-effective membranes will increase the scope of SGE recovery which is not restricted to the naturally occurring salinity gradients.

This study required various spatial datasets and the reason for using the datasets is given in Table 2.

Table 2 Purpose of different datasets used in the study

Data variable	Purpose
Precipitation (P)	To see the spatial distribution of precipitation over Africa for identification of areas with low precipitation. Precipitation was the input for the RET-P map to identify areas with RET>P. Precipitation was also used in water balance (see section 3.1)
Reference Evapotranspiration (RET)	To see the spatial distribution of RET over Africa for identification of areas with high evapotranspiration. RET was the input for the RET-P map to identify areas with RET>P. RET was also used in water balance (see section 3.1)
Elevation	High elevations require added investments due to transportation costs. Elevation threshold (<15 meters above sea level) was chosen to identify low-lying areas.
Slope (derived from elevation)	Steep slopes are unsuitable for transport of seawater to evaporation pond and such areas need extensive land-levelling work which increases project expenditure. Slope threshold (<3°) was used for this study
Landcover	Landcover was used to include areas with bare/sparse vegetation and avoid croplands, built-up areas, water bodies and important ecosystems.
Sea Surface salinity	It is essential to determine the salinity of evaporation pond which is unknown ..(6). It is also the important variable in ..(1) which is used to estimate the potential energy
Sea Surface temperature	It is essential to estimate the theoretical energy ..(1)

3.1 Theoretical potential energy

For this study, an artificial and hypothetical wetland is used as an evaporation pond to generate salinity gradient between the seawater and the pond. Although the first step in this study is the identification of the suitable sites for evaporation pond, it is important to know the theoretical approach used in this study related to the salinity gradient principle. This section describes the steps used to estimate the theoretical potential energy estimate from the evaporation pond.

The amount of potential energy that can be gained from salinity gradient depends on sea salinities and temperature of the mixing solutions and the inflow of diluted solution (Kuleszo et al., 2010). The theoretical potential can be calculated using equation 1 which based on Gibb's free energy equation (Emdadi et al., 2016)

$$U = Q_{in} \times 2RT \left(\left(C_D \ln \frac{2C_D}{C_D + C_C} \right) + \left(C_C \ln \frac{2C_C}{C_D + C_C} \right) \right) \quad ..(1)$$

Where, U is theoretical potential SGE (J/s), Q_{in} is inflow rate (m^3/s) of the dilute solution (seawater), T is temperature (K), C_D is concentration of salt in diluted solution (mol/m^3), C_C is concentration of salt in concentrated solution in (mol/m^3) and R is the universal gas constant ($8.314 J/(mol.K)$).

Thus, for estimation of the theoretical potential energy, temperature, the flowrate of the diluted solution (Q_{in}) and salinities of the diluted and concentrated solutions are important variables.

In this study, the values and inflow (Q_{in}) and the outflow (Q_{out}) rates of water from the pond will be determined by using the water balance approach. Furthermore, the salinity of the pond (C_C) can be estimated from the water and salt balance approach described in the following sections.

3.1.1 Water balance and salt balance

The general water balance equation is given as:

$$dS = Q_{in} - Q_{out} + (P - ET - I) \quad ..(2)$$

Where, dS is the change in storage, Q_{in} and Q_{out} represent the inflow and outflow (m^3/s), here for the evaporation pond which can be controlled by pumps. P is the total precipitation rate on the lake (m^3/s), ET is the rate of evapotranspiration from the whole lake (m^3/s) and I is the infiltration. Figure 5 shows the conceptual diagram for theoretical evaporation pond.

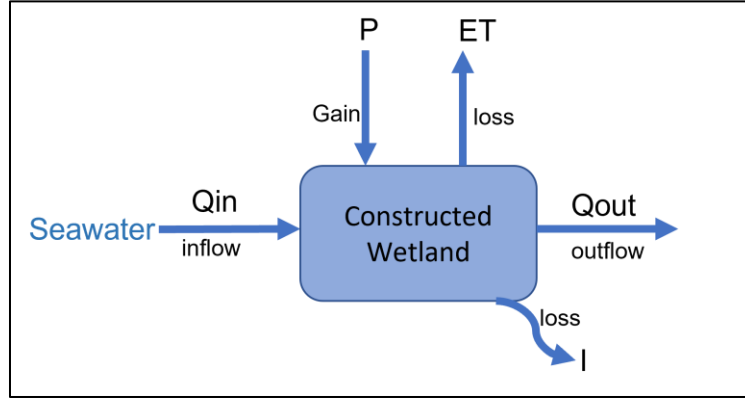


Figure 5: Conceptual diagram for the water balance in the evaporation pond

Here, the pond is assumed as a steady state system and all the balance equations are done for steady state condition and losses due to infiltration are considered as zero. In steady state conditions, there exists an equilibrium in the terms of water balance, therefore, the $dS=0$, and thus the equation 2 can be written as

$$Q_{out} = Q_{in} + (P - ET) \quad ..(3)$$

Here, the values for P and ET for the study area are obtained from spatial datasets. Rearranging equation 3, the difference between P and ET should be equal to the difference between Q_{in} and Q_{out} . To estimate the maximum potential gain, Q_{in} will be varied to assess the ideal combination for maximum potential gain in ponds of different area sizes. Q_{out} can be obtained from equation 3. Since the values of precipitation, evapotranspiration, temperature, and salinity of seawater are actual values in the study area obtained from spatial datasets, only Q_{in} and Q_{out} can be varied to determine the salt concentration in the pond which is used in equation ..(1 to estimate the potential energy.

The salt balance is given by the equation

$$Q_{in} \times C_D = Q_{out} \times C_C + (P - E) \times C_W \quad ..(4)$$

Where C_D is the salinity of sea water, C_C is the concentration of salt in the evaporation pond and C_w the salinity of $(P-E)$ in mol/m^3 .

Considering the precipitation and evaporation as (by approximation) pure water, $C_w=0 mol/m^3$, the equation 4 can be rewritten as

$$Q_{in} \times C_D = Q_{out} \times C_C \quad ..(5)$$

Thus, the salinity of the evaporation pond can be given by

$$C_C = \frac{Q_{in}}{Q_{out}} \times C_D \quad ..(6)$$

Using the above equation, the equilibrium salt concentration in the evaporation pond can be calculated. This can be used to determine the potential energy gain from the pond using equation ..(1).

Thus, this study focuses on using the water and salt balance approach to determine the potential energy from an artificial pond. The feasible sites for the location of the pond were identified in Africa for which the methodology is described in the following sections.

3.2 Study area

Africa, the second largest continent in the world, comprises 54 countries and has a population of 1.4 billion which is equivalent to 16.72% of the total world population (*Population of Africa (2022) - Worldometer, 2022*) and it is likely to double by 2050 (Doorga et al., 2022). The population growth will lead to increase in energy demands. Currently, the electricity generation in Africa is heavily reliant on fossil fuels (40% Natural gas, 30% coal and 90% Oil) and the renewable energy mainly from hydropower, solar, wind and geothermal (IEA, 2019). However, hydropower needs alternative options as water resources are limited in Africa with high frequency of droughts. SGE generation using river water is challenging not only due to limited freshwater resources but also because of transboundary rivers which may create political disputes. Thus, the proposed method of using seawater-evaporation ponds for SGE in Africa is promising as it does not involve use of transboundary water bodies. Moreover, the evaporation ponds are feasible due to low precipitation and high evaporation in many parts of Africa (See 10, Figure 16 and Figure 17). Furthermore, the feasibility of renewable energy depends upon several geographical, environmental, and political factors and thus it is important that investments for renewable energy are made at appropriate locations. Thus, this study also focuses on identifying suitable area for the evaporation pond in Africa.

3.3 Data description and preparation

This section describes the raster and vector datasets used in the study. The purpose of each data variable is already mentioned in Table 2. The raster datasets for precipitation, evapotranspiration, sea surface temperature and sea surface salinity were acquired for the year 2019. The land cover dataset is a product from ESA which is provided for the year 2020. Table 3 provides the general characteristics of the datasets and a brief description of the datasets is given below.

3.3.1 Raster Data

- **Precipitation**

The daily files for the GPM IMERG final precipitation (Huffman et al., 2019) were downloaded from the GPM directory (<https://disc.gsfc.nasa.gov/>) in NetCDF format. The Final Run Daily product is derived from the half hourly product by summing the valid retrievals for the day and the unit is mm (equivalent to kg/m²). The daily precipitation files were summed to obtain the total annual precipitation (mm/year) and then clipped to the extent of the Reference Evapotranspiration (RET) dataset. Further the annual data was downscaled to match the resolution of the RET dataset (0.17°) using the bilinear interpolation method which is recommended for continuous datasets such as precipitation (Saleh et al., 2018; Ulloa et al., 2017) as the output cell value is assigned a new value by taking the weighted average of the four bordering cells. Since the RET, elevation and land cover datasets are in GeoTIFF format, the annual precipitation file was converted from NetCDF to GeoTIFF for ease of further analysis.

- **Evapotranspiration**

The annual Reference EvapoTranspiration (FAO, 2020) was obtained from the Water Productivity through Open Access of Remotely sensed derived data (WaPOR) datportal (<https://wapor.apps.fao.org/>) in GeoTIFF format. This portal by Food and Agricultural Organization (FAO) provides spatial data over Africa and the Near East for different variables related to land and water for agricultural productivity. The annual product

has a higher quality due to the gap filling and interpolation methods. The annual RET is obtained by summing the daily RET giving the result in mm.

- **Elevation and slope**

The Shuttle Radar Topography Mission (SRTM) provides Digital Elevation Data (DEM) at 90 m resolution (Reuter et al., 2007) which was used in the study. The data was downloaded through Google Earth Engine (GEE) as GeoTIFF image for Africa. The slope in degrees was generated from the elevation data for further analysis.

- **Land cover**

The landcover dataset used in this study was obtained from (<https://esa-worldcover.org/>) which provides a global land cover product with 11 classes at 10m resolution for the year 2020 derived from Sentinel 1 and 2 (Zanaga et al., 2021). Due to the large data size, the data was obtained only for the potential study sites in Africa which are described further chapters. The landcover data was resampled to 90m using the nearest neighbor method. It was used along with elevation and slope rasters to create a suitability map.

- **Sea Surface Temperature**

The level 4 sea surface temperature was obtained from the project Group for High Resolution Sea Surface Temperature (GHRSSST) which is provided by the UK Met office in netCDF4 format for the year 2019 (Chin et al., 2017). The Operational Sea Surface Temperature and Sea Ice Analysis (OSTIA) daily files were obtained only for the potential sites from (<https://podaac.jpl.nasa.gov/dataset/OSTIA-UKMO-L4-GLOB-v2.0>). The daily files were used to obtain the annual mean temperature which was used throughout the study.

- **Sea Surface Salinity**

The salinity data was obtained from the Barcelona Expert Center (BEC) which provides salinity products derived from the SMOS data (Olmedo et al., 2021). For the coastal areas, radio frequency interferences affect the quality of SMOS observations because the sources emit in the wavelength range where SMOS measures and are much stronger than the small signals from ocean and land surfaces. The data from BEC cope with land and radio frequency contamination thus making the data appropriate for the coastal areas. The daily L4 Sea Surface Salinity (SSS) product which has been validated using the Argo near-surface measurements was obtained for the year 2019 from (<http://bec.icm.csic.es/>). The daily files were used to obtain the annual mean salinity which was used throughout the study.

3.3.2 Vector data

The shapefile for Africa boundary was used to clip raster datasets to Africa which was obtained from ICPAC geoportal.

Table 3 Summary of the datasets used in the study

Variable	Source	Spatial and temporal resolution	Platform/Sensor	Time span
Precipitation	NASA GPM IMERG Final Run	0.1° x 0.1°, Daily	https://gpm.nasa.gov/resources/documents/algorithm-information/IMERG-V06-ATBD	2000 June- Sep 2021
Reference Evapotranspiration	FAO WaPOR	0.17°, Annual	MERRA/GEOS-5, MSG	2009 January- Present
Elevation	NASA/CGIAR	90 m	SIR-C	2018-Nov- Present
Landcover	ESA WorldCover	10 m	Sentinel-1 and 2	2020
Sea surface temperature	UK Met Office	0.05°, Daily	GOES-16 / ABI TRMM / TMI MSG2 / SEVIRI NOAA-20 / AVHRR-3 METOP-A / AVHRR-3	2006-Dec-31 to Present
Sea surface salinity	BEC	0.05°, Daily	SMOS/MIRAS	2011-2019

3.4 Site suitability

3.4.1 RET -P and coastal proximity

For the specific site selection, the main criteria for choosing the potential sites were that the annual RET should be greater than the annual precipitation. For this purpose, a map of RET – P was generated in QGIS using the raster calculator. The areas with RET- P > 0 and RET > 2000 mm/year were identified. Furthermore, as seawater is the source of inflow for the pond, area near the coast is preferred. A buffer of 100 km was applied from the African coastline to ensure the proximity to the seawater since it will reduce the energy and costs for pumping seawater in the evaporation pond. Figure 6 shows the 5 potential sites selected for further analysis based on the RET-P calculations and the coastal proximity.

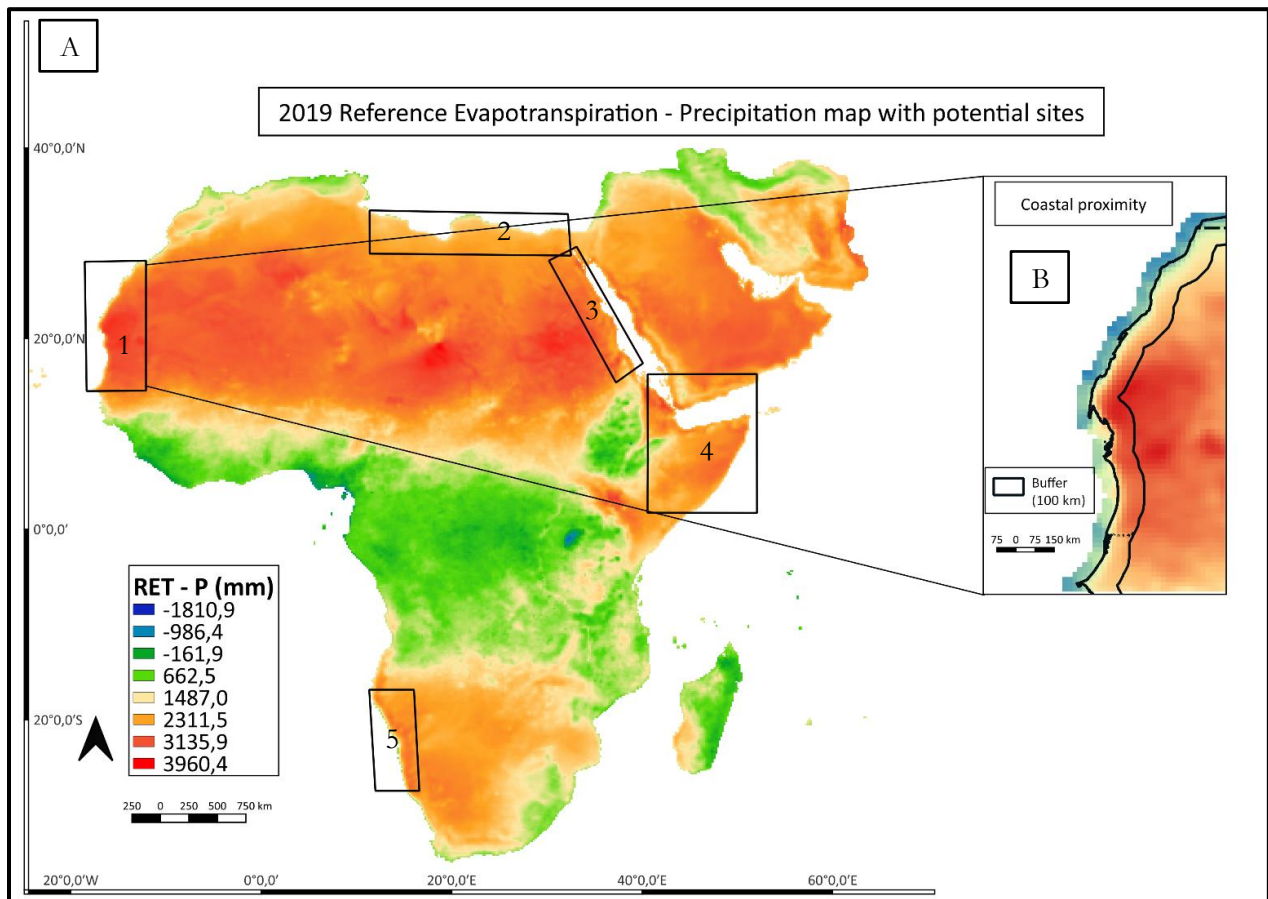


Figure 6: (A) RET-P map with the locations of 5 sites (B) Site 1 showing the 100 km coastal proximity

3.4.2 Elevation, slope and landcover

The elevation and slope analyses are important for identifying flat areas which are suitable for development of evaporation ponds. Furthermore, low lying lands with flat terrain are preferable for pumping of seawater in the pond. Table 1 shows the maximum and minimum values of elevation and slope in the areas and the criteria for selecting flat areas from the five sites. The landcover is also an important criterion to know the agricultural and built-up areas which cannot be used as a location for the pond. Moreover, landcover was used to eliminate sites with permanent water bodies and important ecosystems like mangroves and grasslands. As most of the sites lie in Saharan region, they majorly have bare/sparse vegetation cover as seen in Figure 7, except a few areas which covered with mangroves, croplands and built-up areas like cities and roads. To avoid the latter landcover areas, all the landcover classes apart from bare/sparse vegetation were excluded for the site suitability analysis.

Table 4: Elevation and slope for the five sites

Site	Elevation (m)		Slope (degrees)		Criteria for site selection
	Minimum	Maximum	Minimum	Maximum	
1	-67	367	0	27	Elevation \leq 15 AND Slope \leq 3
2	-82	1401	0	50	
3	-5	2683	0	68	
4	-100	2309	0	55	
5	-168	2400	0	52	

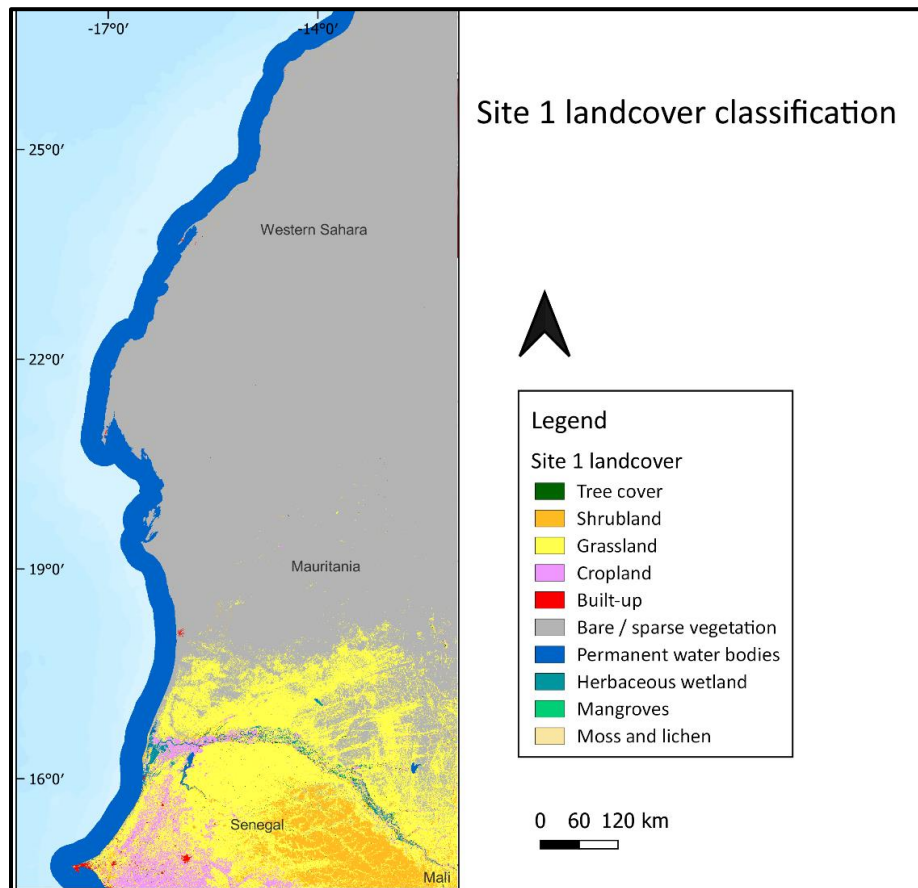


Figure 7: Landcover classification- site 1

Using the criteria mentioned above for elevation, slope and landcover, the suitability maps for all the sites were prepared and locations for the theoretical ponds were marked in these sites. Based on the suitable area in each site, a pond of minimum 100 km² was marked to estimate the potential energy gain by creating grids of 10 km × 10 km for all the sites. The sites lacking uninterrupted suitable areas (≥ 100 sq km) for construction of the pond were excluded from further analysis for the estimation of energy gain.

3.5 Estimation of SGE potential

The mean precipitation and evapotranspiration data for the evaporation pond area marked at the 5 sites was obtained using zonal statistics tool in QGIS. This tool provides statistics like mean, median, maximum, minimum, standard deviation etc. for pixels of a raster that are within a polygon in vector layer. Table 5 shows the sizes of ponds at each site and the mean values for the required variables were obtained for these area sizes. Sites which did not have uninterrupted areas for pond are marked as NA. Furthermore, the corresponding values for sea surface salinity and temperatures were also obtained by using the same tool.

After getting all the required values, the salinity for all the ponds was obtained individually using the water and salt balance approach as described in section 3.1.1. The theoretical potential energy for each pond was calculated using ..(1).

Table 5 Area size of ponds at the 5 sites

Site	Area size (km ²)
Site 1	108.74
	217.98
	434.61
	1307.21
Site 2	219.599
	283.92
Site 3	NA
Site 4	109.342
	217.473
Site 5	NA

3.6 Uncertainty propagation for potential SGE

The potential SGE is derived from many parameters $..(t)$ like T, Q_m, C_D and C_C . To calculate the uncertainty of U , the law of uncertainty propagation was applied to find error propagation of different variables involved in calculation of U .

The value of Q_m is derived from P and RET . The value for uncertainty for P and RET was assumed to be 5%. Firstly, the uncertainty of Q_m , which arises from P and RET was calculated by taking the uncertainty for $P-RET$

$$\sigma Q_{in} = \sqrt{\left(\frac{\partial Q_{in}}{\partial P} \sigma P\right)^2 + \left(\frac{\partial Q_{in}}{\partial RET} \sigma RET\right)^2} \quad ..(7)$$

$$\sigma Q_{in} = \sqrt{(1 \times 0.05)^2 + (1 \times 0.05)^2} \quad ..(8)$$

$$\sigma Q_{in} = 0.071 \text{ m}^3/\text{s}$$

The uncertainty of Q_m from equation 8 was used for calculating the uncertainty in the U . The value of universal gas constant is always the same and the error associated with it is negligible as compared to other errors. Hence, it was not included in the uncertainty calculations for U .

Similar to equation $..(7)$, the uncertainty for U was calculated as shown below

$$\sigma U = \sqrt{\left(\frac{\partial U}{\partial Q_{in}} \sigma Q_{in}\right)^2 + \left(\frac{\partial U}{\partial T} \sigma T\right)^2 + \left(\frac{\partial U}{\partial C_D} \sigma C_D\right)^2 + \left(\frac{\partial U}{\partial C_C} \sigma C_C\right)^2} \quad ..(9)$$

σ denotes the uncertainty equation $..(9)$ describes the propagation of the uncertainty into the power generation, assuming all uncertainties of the inputs are independent from each other.

The uncertainty in T was taken 0.1 which is given in the GHRSSST Data Specification (<https://www.ghrsst.org/documents/q/category/gds-documents/operational/>) and for the other variables as 0.5.

The uncertainty value for U was ± 0.1 (10%) J/s.

4. RESULTS

4.1 Site suitability

Based on the variables considered for identification of suitable areas for development of evaporation ponds, 5 sites were chosen as potential areas. The suitability maps for the five sites are described in this section. Overall, site 1 had the most and largest suitable areas, while site 3 and site 5 did not have continuous suitable area for evaporation pond. As described in section 3.5, the potential energy estimates are calculated over different pond sizes however, the maps show the location and area of the largest pond marked in that site. In all the sites, orange indicates unsuitable areas while green indicates suitable area for evaporation pond.

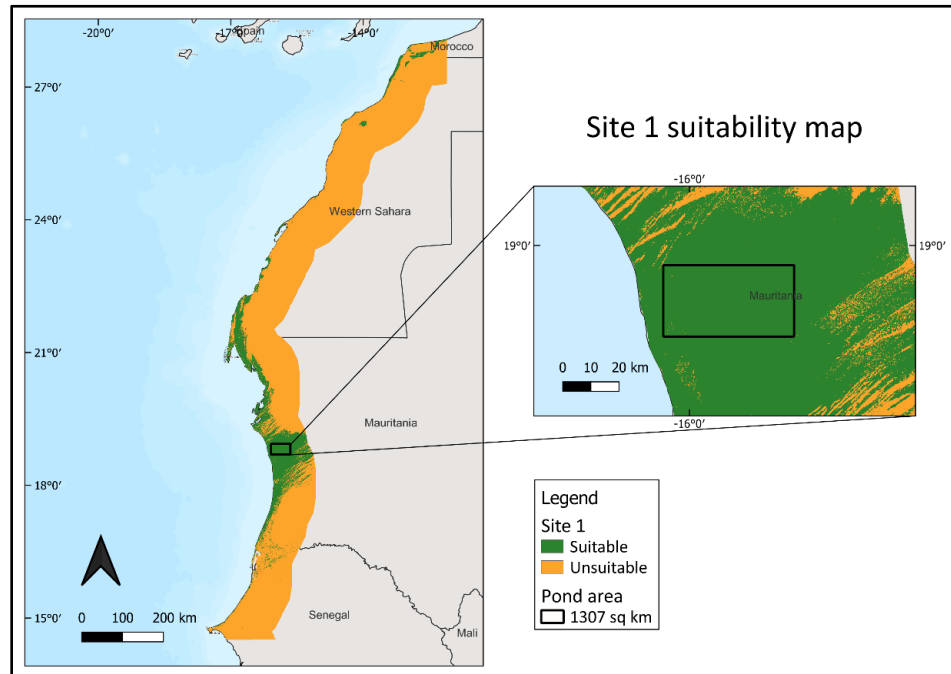


Figure 8: Site 1 suitability map

Site 1 (Figure 8) had more suitable area as compared to the other sites. The elevation and slope values in site 1 lie lower range (Table 4) than the other sites which indicate presence of low-lying flat areas with gentle slopes which are suitable. Moreover, the major landcover in site 1 is bare/sparse vegetation which is a positive criterion for pond suitability. Majority of the suitable area lies in Mauritania while Morocco, Western Sahara and Senegal have some specks in the coastal regions. The small patches although suitable do not have sufficient area for a pond of minimum 100 km².

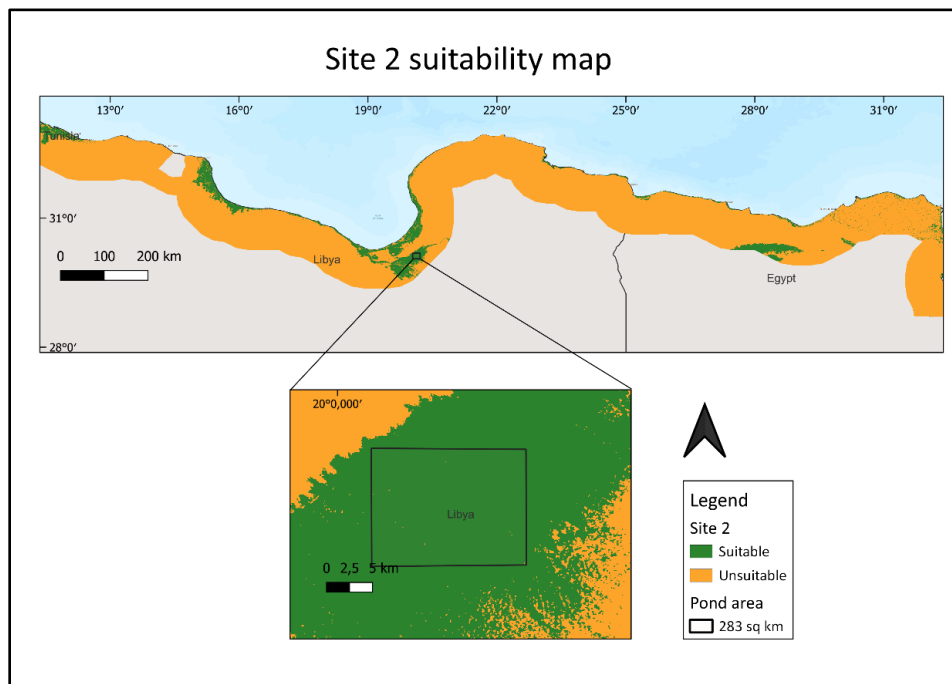


Figure 9: Site 2 suitability map

Site 2 which is in North African countries Libya and Egypt has some small suitable areas bordering the coast but are not large enough to build a pond. Figure 9 shows the location of the pond of 283 km² which approximately 50 km from the coast. The unsuitable area in northeast of Egypt is due to the presence of built-up areas and croplands around the Nile delta. Although there is some area close to the coast in Libya, it is interrupted by cities due to which building a pond is not feasible. Hence, the location of the pond area for this site was chosen inward from the coast away from the settlements.

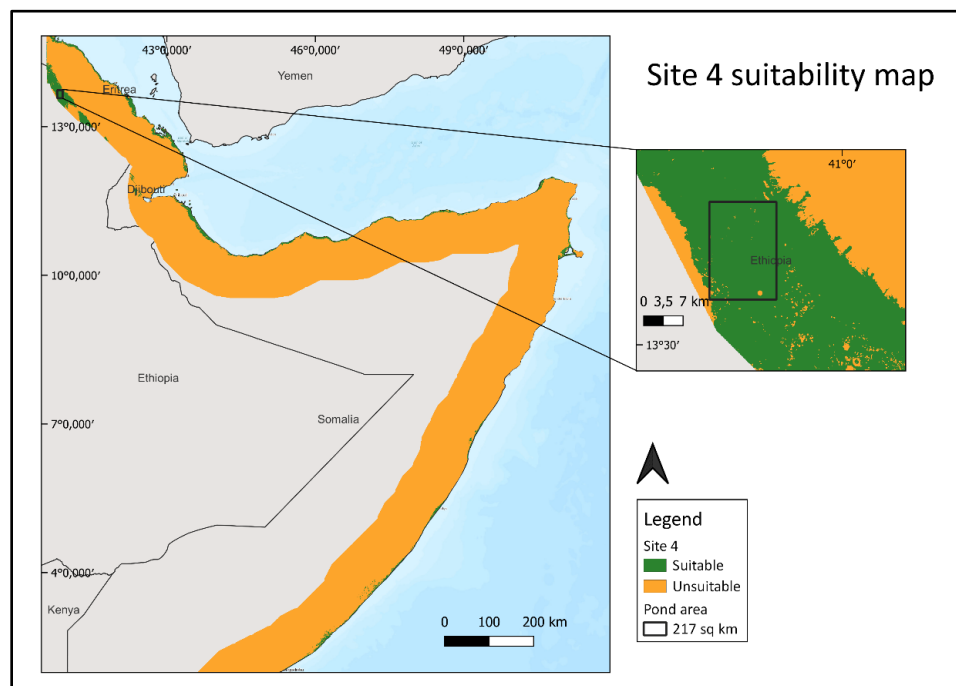


Figure 10 Site 4 suitability map

Site 4 (Figure 10) is spread over four countries Eritrea, Ethiopia, Djibouti, and Somalia. Most of the suitable area lies in Ethiopia, close to the Ethiopia-Djibouti border. The horn of Africa has negligible suitable area, and

a relevant size pond cannot be constructed in such small patch. At the fringes there is a continuous strip of suitable land especially in Eritrea and Djibouti again which is not large enough to build a pond. Thus, the location of pond in this site, like site 2 was chosen inward from coast. The unsuitability of the area is due to high elevation values (see Table 4) attributed to the presence mountainous regions in all these countries.

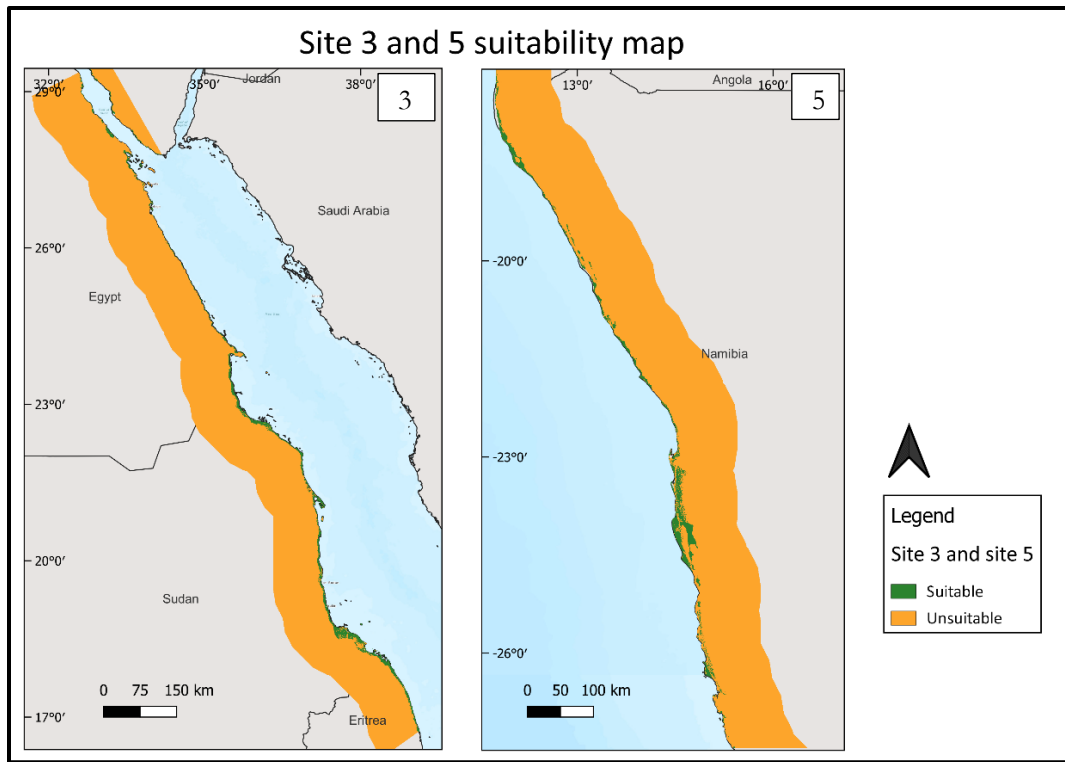


Figure 11 Site 3 and 5 suitability maps

Figure 11 shows suitability maps for site 3 and 5 which are in the northeast and southwest of Africa, respectively. The high elevation values at both the sites due to the mountains like Emba Soira, Eritrea (site 3) and Brandberg mountain in Namibia (site 5) render majority of the area in these both sites unsuitable. Furthermore, presence of some coastal cities in Sudan and Egypt along with croplands in Site 3 limits the suitability. In both these sites a continuous suitable area was unavailable for an evaporation pond. Hence, both these sites were not considered while estimating the potential SGE.

In the next section, the energy estimations from sites 1, 2 and 4 for each pond are presented.

4.2 Theoretical SGE energy potential

The average values for variables required to calculate U in site 1, site 2 and site 4 were obtained as described in section 3.5. This section describes the potential energy estimations with different parameters such as area of the pond, combination of Q_{in} and Q_{out} and salinities of the seawater and pond. Table 6 shows in detail the all the above variables and the corresponding energy at each site. Overall, the highest estimation of potential SGE was from high pond salinities, large areas and low Q_{in}/Q_{out} combinations.

Table 6: Theoretical SGE potential for each pond

Site	Pond area (m ²)	Q _{in} factor (a)	Q _{in} [a×(P- RET)] (m ³ /s)	Q _{out} (m ³ /s)	SST (K)	C _D (mol/m ³)	C _c (mol/m ³)	Energy (MW)
1	108,774,000	2	20.55	10.28	294.4	501.5	1003	8.57
		1.5	15.41	5.14			1504.5	19.79
		1.3	13.36	3.08			2173.16	36.82
		1.2	12.33	2.06			3009	59.97
		1.1	11.30	1.03			5516.5	135.30
	217,983,000	2	40.52	20.26	294.3	500.9	1001.8	16.87
		1.5	30.39	10.13			1502.7	38.97
		1.3	26.34	6.08			2170.5	72.50
		1.2	24.31	4.05			3005.4	118.07
		1.1	22.29	2.03			5509.9	266.36
	434,611,000	2	82.58	41.29	294.3	500.9	1001.8	34.39
		1.5	61.93	20.64			1502.7	79.43
		1.3	53.67	12.39			2170.56	147.76
		1.2	49.55	8.26			3005.4	240.62
		1.1	45.42	4.13			5509.9	542.84
	1,307,271,000	2	260.27	130.14	294.5	502.3	1004.6	108.75
		1.5	195.20	65.07			1506.9	251.19
		1.3	169.18	39.04			2176.63	467.25
		1.2	156.16	26.03			3013.8	760.91
		1.1	143.15	13.01			5525.3	1716.54
2	219,599,000	2	30.39	15.20	294.3	522.8	1045.6	13.21
		1.5	22.79	7.60			1568.4	30.51
		1.3	19.75	4.56			2265.46	56.76
		1.2	18.23	3.04			3136.8	92.43
		1.1	16.71	1.52			5750.8	208.52
	283,920,000	2	39.40	19.70	294.5	524.9	1049.8	17.20
		1.5	29.55	9.85			1574.7	39.74
		1.3	25.61	5.91			2274.56	73.93
		1.2	23.64	3.94			3149.4	120.40
		1.1	21.67	1.97			5773.9	271.61
4	109,342,000	2	21.04	10.52	301.6	600.9	1201.8	10.77
		1.5	15.78	5.26			1802.7	24.88
		1.3	13.67	3.16			2603.9	46.29
		1.2	12.62	2.10			3605.4	75.38
		1.1	11.57	1.05			6609.9	170.07
	217,473,000	2	41.84	20.92	301.7	601.7	1203.4	21.46
		1.5	31.38	10.46			1805.1	49.57
		1.3	27.20	6.28			2607.3	92.20
		1.2	25.10	4.18			3610.2	150.16
		1.1	23.01	2.09			6618.7	338.74

4.2.1 Potential SGE and salinity of pond

SGE mainly depends on the salinity gradient ΔS , thus higher salinity gradient will result in higher values of energy. The results in

Table 6: Theoretical SGE potential for each pond show increasing values of potential SGE with increasing salinity gradient. The salinity of the pond is mainly dependent on C_D , Q_{in} and Q_{out} ..(6). The salinity of seawater at site 1 was between 501-503 mol/m³ (~35.7 PSU) which is the typical salinity of seawater. However, site 2 and site 4 had higher salinities in the range of 522-525 mol/m³ and 600-602 mol/m³ respectively (~37-38 PSU) which are also higher than the typical salinities of seawater. Hence, site 2 and site 4 also had higher salinities for the evaporation pond as compared to site 1. The salinity gradient increases with decreasing Q_{in} factor as seen **Error! Reference source not found.** which shows salinity of largest pond at every site. Thus, to gain more energy while keeping the area constant, only the values for Q_{in} and Q_{out} can be varied to get the optimal salinity gradient since the salinity of the seawater is fixed for a certain area.

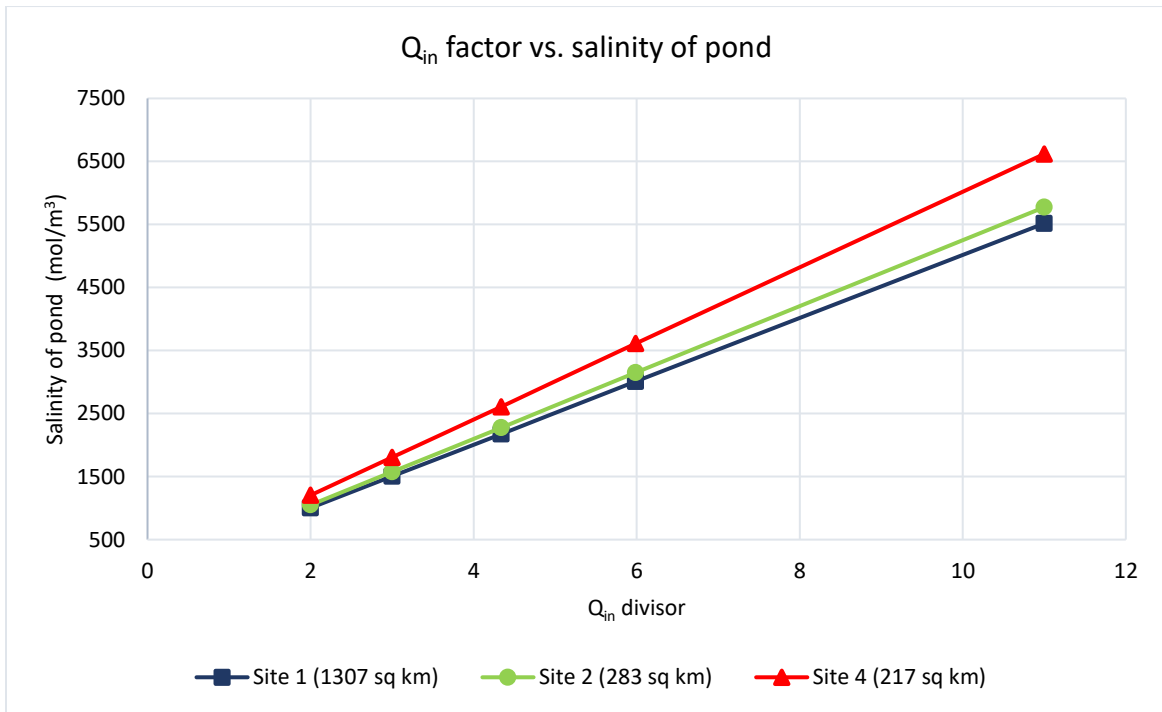


Figure 12: Q_{in} factor vs salinity of largest pond at every site

4.2.2 Potential SGE and area of pond

Although site 1 has lower salinity values, it has the maximum estimation for potential SGE amongst all the sites. This is due to the area of pond size. Site 1 had the biggest potential pond area (1307.2 km²) with potential SGE 1716.54 MW. Table 6 shows that the highest potential SGE in each site is from the largest pond in that area. Table 7 shows the percent increase in energy due to the percent increase in the area. The percentage energy gain was calculated with respect to smallest pond area at the site. Furthermore, the values are compared only for the highest potential SGE in each area highlighted in Table 6. For site 1, the area increases of 100 % shows energy gain of 97%. Thus, the ratio between pond area rise and energy gain is ~1:1.

Table 7: Relationship between area change and energy gain

	Area change (%)	Energy gain (%)
Site 1	100%	97%
	300%	301%
	1102%	1169%
Site 2	29%	30%
Site 3	99%	99%

4.2.3 Potential SGE and Q_{in} , Q_{out}

Table 6 shows the highest potential SGE at each site for the lowest factor of Q_{in} . At all the sites the maximum energy possible was for the Q_{in} factor of $1.1 \times (P-RET)$ while the minimum energy was for the Q_{in} factor of $2 \times (P-RET)$. The plots (Figure 13-Figure 15) below are for the largest pond at every site and show the potential SGE with respect to Q_{in} and Q_{out} . For the other sites the plots are provided in Appendix (Figure 18-Figure 21). In every case, potential SGE is increasing with decreasing values of Q_{in} and Q_{out} . Furthermore, as stated in section 4.2.1, Q_{in} and Q_{out} also play an important role in influencing the salinity of the pond which ultimately influences the potential SGE. The salinity of the pond is determined by Q_{in} and the plots below show the dependence of SGE to this influx. When $Q_{in} = P-RET$, Q_{out} becomes zero. Thus, the evaporation pond with no outflow will ultimately result in salt crust if all water is lost to evaporation. Furthermore, if $Q_{in} > 2 \times (P-RET)$, the salinity gradient is small which will give very low estimations of energy. The Q_{in} factor of 1.1 yields the maximum U (Table 6). If Q_{in} is factor is taken below 1.1 the salinity of pond increases to values which are not practical to maintain in the evaporation pond. Hence, the Q_{in} factor was varied only between **2-1.1** to calculate theoretical SGE potential.

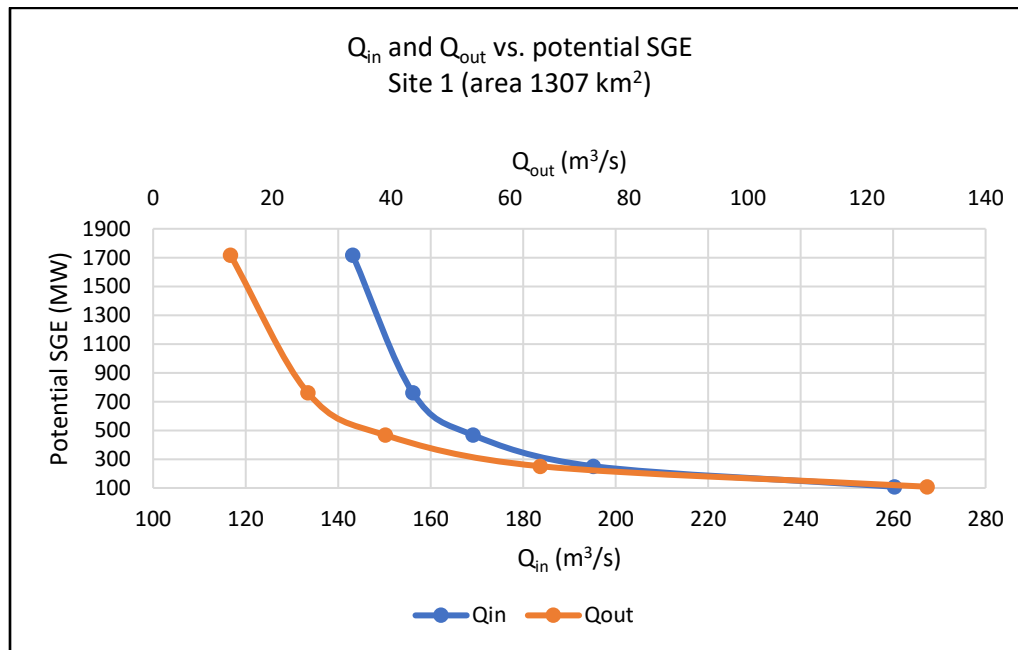


Figure 13: Q_{in} and Q_{out} vs. potential SGE for area of 1307 km² in site 1

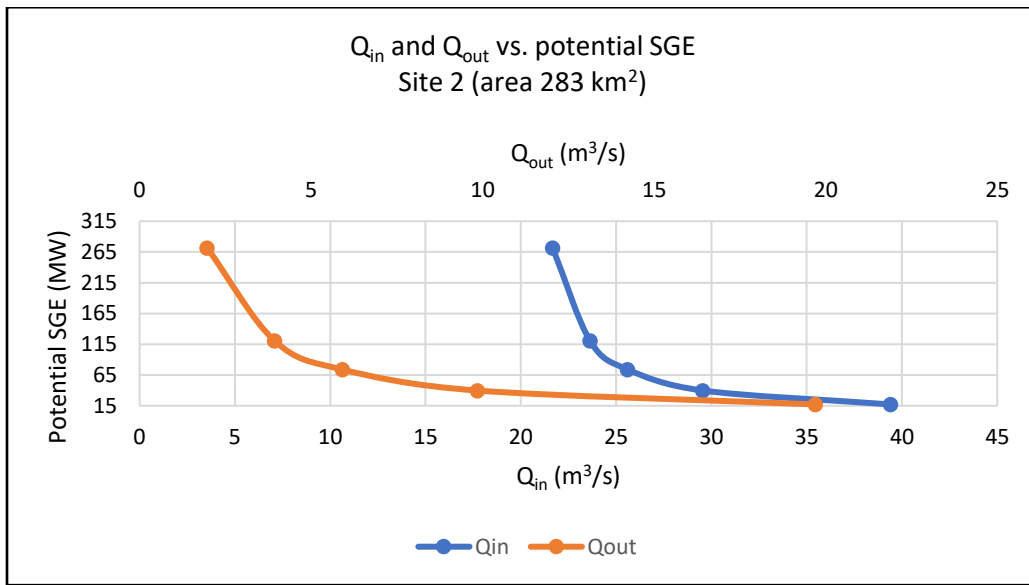


Figure 14: Q_{in} and Q_{out} vs. potential SGE for area of 283 km² in site 2

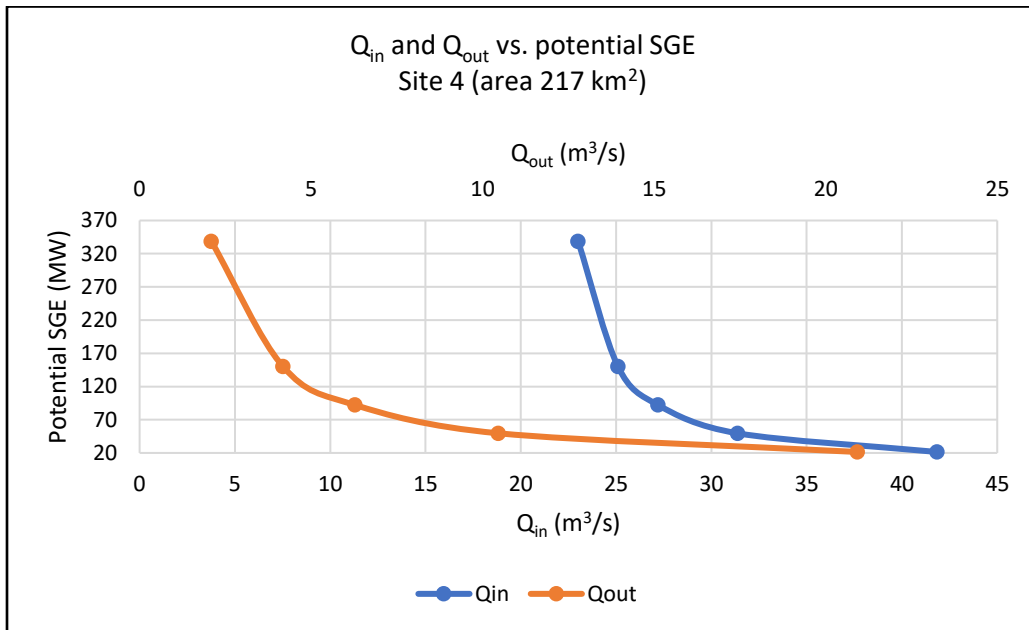


Figure 15: Q_{in} and Q_{out} vs. potential SGE for area of 217 km² in site 4

5. DISCUSSION

5.1 Site specific SGE potential

Initially five sites were identified as potential locations for the evaporation pond out of which two sites (site 3 and site 5) were excluded from the potential SGE estimations due to lack of a sufficiently large suitable area. Site 1, located in northwest Africa, had the largest pond of all the three remaining sites as well as the highest U (1716.54 MW). Furthermore, the location of the evaporation pond at site 1 is closer to the coast as compared to the other two sites. Thus, a SGE plant built at site 1 will have reduced energy and costs for pumping seawater to the evaporation pond due to its proximity to the coast as compared to the other sites. The evaporation pond is located close to Nouakchott, the capital city of Mauritania which is an important economic center with a deepwater port and international airport. An SGE plant built here would provide clean energy which can be

utilized for commercial as well as household purposes. The location of evaporation ponds at sites 2 and 4 is inshore with some unsuitable areas between the coast and the ponds. The unsuitable areas could be due to high elevation or steep slopes. In such cases, although there is a feasible area that can be used for evaporation pond, the transport of seawater to the pond will consume more energy due to elevation changes. The unsuitable areas in between could also be due to unsuitable landcover like croplands or tree cover making the transport of seawater a challenging process. The nearest urban area near the evaporation pond in site 2 is Ajdabiya, an important town in Libya. However, the highest theoretical SGE from this site is 271.61 MW and the energy that could be actually obtained will fall far below this value considering factors like energy inputs for water transfer to the plant, membrane costs, and operating costs. Site 4 evaporation pond also does not have high potential energy due to the small pond size. Considering the technical potential to be substantially lower than theoretical SGE, building a pond at these two sites will not be affordable.

5.2 Comparison with other renewable energies

The true potential of the salinity gradient energy can only be understood after comparing it with other sources of renewable energy. Currently, Africa has no existing SGE plant and hence all the comparisons are based on theoretical SGE. Africa has a large solar deposit; thus, it will be relevant to first compare SGE to solar energy and then to other the other sources.

5.2.1 Solar energy

The SGE from each site has been compared to potential or practical solar energy calculations from literature for the same areas. Nouakchott, Mauritania which is located near site 1 evaporation pond has the largest operational solar plant in Africa. It produces 15 MW which can satisfy 10% of the energy requirements of Nouakchott (El Hacen Jed et al., 2020). This value is quite lower than the theoretical SGE from evaporation pond (1716.54 MW) and even after considering the technical potential the SGE will be more. The advantage of the solar plant over evaporation pond is low land requirement and developed technology which will make solar energy less expensive than SGE. A study conducted to identify solar power potential sites in East Shewa, Ethiopia (Gerbo et al., 2020), which lies close to site 4 estimated 2.2×10^6 MW energy can be obtained from an area of 564 km² which is much higher than the maximum theoretical SGE at this site. Finally, for site 2 which is in Libya the theoretical SGE is more than some photovoltaic (PV) projects planned in the country (Maka et al., 2021). PV projects with power between 40 MW and 100 MW have been planned in different cities of Libya. Considering the technical SGE potential to be 50% of the theoretical SGE, the highest energy estimation is approximately 135 MW which is higher than the energy obtained from PV. Thus, site 1 and site 2 would generate more SGE as compared to PV, however at site 4 the energy from PV is more.

5.2.2 Wind energy

A 30 MW wind farm is operational near Nouakchott city in Mauritania since 2015. The farm provides 5.073×10^5 MWh to the power grid (Heiba et al., 2021). This value is based on the operating hours of the wind farm and a relevant comparison to potential SGE at this site is not possible. The wind potential in three regions of Libya including Tripoli, the capital city was assessed by (Kassem et al., 2019). The maximum wind potential from a single windmill in the three regions was in the range of 0.991 MW to 1.5 MW. However, the total power from these wind farms depends on the number of windmills. The exploitable potential wind power in Ethiopia is 10,000 MW (Asress et al., 2013) however the operational wind farms have capacity of 52 MW. An area of 401 km² can be used to construct 2005 MW wind farm. Theoretical SGE estimate from evaporation pond of 217 km² in Ethiopia (site 4) was 338.7 MW. The technical potential is below this value and a similar size area would have lower SGE potential than wind power.

Although the above comparisons give some idea about status SGE compared to PV and wind other factors like operation costs, energy costs, life cycle of the plant and area footprint should be considered for a detailed comparison. Moreover, the other sources of energy are already in operational stages while the SGE estimations

remain at theoretical level. Thus, the practical limitations and advantages of a fully functioning PRO/RED-SGE plant cannot be assessed.

5.3 Advantages and limitations of SGE in evaporation ponds

The main advantage of extraction of SGE from evaporation ponds is that it does not pose a threat to valuable freshwater resources. Compared to river-seawater SGE systems, this system remains unaffected by the temporal inconsistency of the inflow as seawater, unlike river water, is abundant. Moreover, the filling of evaporation ponds can boost the rainfall in the region due to increased evaporation from the pond water. The land requirements for evaporation ponds are large, however they can serve other purposes like usage of the pond for salt production. The saline ponds could be used as ecological recreational site to introduce flora and fauna suitable to highly saline ecosystems. Moreover, setting up resorts and fishing villages could boost the economy through recreational methods and cover some operating costs for the SGE plant.

In this study the infiltration losses from pond were not considered which will also affect the theoretical estimations. Furthermore, the energy required for transport of water to the membrane unit needs to be considered while estimating the technical potential. The energy estimations are done using annual mean values for all the parameters. The potential SGE might increase or decrease if the seasonal values are considered and the seasonality of all the variables in reality will affect the efficiency of SGE plant.

The environmental impacts of such a pond should also be considered. The accumulation of salts on land due to seawater transport can hamper the soil quality and in case the plant goes out of operation the land may permanently become saline and unsuitable for other purposes. Currently, this approach is conceptual and needs economic analysis to establish financial viability. It also involves construction of pipelines/canals for seawater transport. Although the canals can be navigable, the implementation costs will be overly high. Furthermore, acquisition of lands will have legal restrictions which need to be considered before making plan for the pond. Lastly, the membrane area and costs also need to be considered and if the membranes become available at industrial level and low cost, such evaporation ponds will be feasible.

6. CONCLUSION

This study was carried out to estimate the maximum potential energy from saline ponds at some suitable sites in Africa. Precipitation, evaporation, elevation, slope, and landcover are important criteria to identify the suitable areas. The flow of Q_{in} and Q_{out} can be controlled within limits, and the maximum energy was calculated for $Q_{in} = 1.1 \times (P-RET)$. For this study, the northwest region of Africa, especially Mauritania was identified as the most suitable area to build an evaporation pond with theoretical estimations of 1716.54 MW. Even if the technical potential is 40-50% of the theoretical potential, an SGE plant in this area would provide significant clean energy. Further estimations for costs of membrane, transportation of water and energy will help to assess the financial viability of this method.

This section also includes answers to research questions in section 1.2

Research question 1: What are the relevant variables to be considered for identifying suitable area for evaporation pond?

For initial suitability assessment, the most important variables to be considered for identification of suitable areas are the higher evaporation rates than precipitation as the salinity in the evaporation pond since evaporation is the main driver for the salinity in the pond. Furthermore, coastal proximity is necessary as seawater is pumped in the pond. Elevation and slope are important to identify low lying areas with gentle slopes. Lastly, landcover is important to exclude waterbodies, croplands, built-up areas and important ecosystems like forests or mangroves.

Research question 2: Where are the suitable areas for energy generation located?

The large suitable areas for evaporation pond are located close to the coast and in the countries Mauritania, Libya, and Ethiopia.

Research question 1: Which combination of parameters is most suitable for energy generation in the artificial wetland?

Since Q_{in} and Q_{out} were the only variables that could be varied, the highest combination of energy was obtained when Q_{in} and Q_{out} values were low. The low values had the theoretical ponds with highest salinities creating large salinity differences in the pond and seawater which led to high energy estimations.

Research question 2: What is the maximum potential energy gain from the artificial wetland?

The maximum theoretical potential energy was 1716.4 MW from the evaporation pond of 1307 km² in site 1. Considering the technical potential to be 40-50% of the theoretical and, the energy obtained is significant and can be used to provide electricity for different activities in the country.

7. RECOMMENDATIONS

In this study, the energy estimations were carried out using open-source remote sensing data. The use of in-situ data, especially for the salinities of seawater will help to validate and improve the accuracy of the energy estimations. The SGE generation majorly depends on the membrane area and density, thus the consideration of these factors will give practical estimations of energy. Most of the studies have applied either PRO or RED method to estimate the theoretical energy and a suitable method for this approach should be identified to suggest the type of plant that can be built for the seawater-evaporation pond system. Furthermore, the pond areas for this study were considered as rectangle and did not include the drainage basin for water accumulation. More realistic results can be generated if water basin and factors like flow direction and flow accumulation are taken into consideration.

8. ETHICAL CONSIDERATIONS, RISKS AND CONTINGENCIES

The research was carried out by using open data sources. The research is a theoretical study to estimate the potential energy and building of the infrastructure is not proposed which would be sensitive for local people or the environment. Thus, use of any sensitive data or ethical requirements like 'consent to publish or participate' are not required. In this research, authenticity and truthfulness will be shown in recording all the data, analysis methods used, findings and underlying assumptions.

9. REFERENCES

- Alvarez-Silva, O., & Osorio, A. F. (2015). Salinity gradient energy potential in Colombia considering site specific constraints. *Renewable Energy*, *74*, 737–748. <https://doi.org/https://doi.org/10.1016/j.renene.2014.08.074>
- Arias, P. A., Bellouin, N., Coppola, E., Jones, R. G., Krinner, G., Marotzke, J., Naik, V., Palmer, M. D., Plattner, G.-K., Rogelj, J., Rojas, M., Sillmann, J., Storelvmo, T., Thorne, P. W., Trewin, B., Rao, K. A., Adhikary, B., Allan, R. P., Armour, K., ... Zickfeld, K. (2019). Foreword Technical and Preface. In *Climate Change and Land: an IPCC special report on climate change, desertification, land degradation, sustainable land management, food security, and greenhouse gas fluxes in terrestrial ecosystems*.
- Asress, M. B., Simonovic, A., Komarov, D., & Stupar, S. (2013). Wind energy resource development in Ethiopia as an alternative energy future beyond the dominant hydropower. *Renewable and Sustainable Energy Reviews*, *23*, 366–378. <https://doi.org/10.1016/J.RSER.2013.02.047>
- Budi, S. H., Susanto, H., & Hermawan. (2021). The potential recovery energy of SWD (sea water desalination) by SGP (salinity gradient power). *Journal of Physics: Conference Series*, *1858*(1), 012078. <https://doi.org/10.1088/1742-6596/1858/1/012078>
- Castelos, M. A. (2014). Marine Renewable Energies: Opportunities, Law, and Management. *Ocean Development & International Law*, *45*(2), 221–237. <https://doi.org/10.1080/00908320.2014.898926>
- Chin, T. M., Vazquez-Cuervo, J., & Armstrong, E. M. (2017). A multi-scale high-resolution analysis of global sea surface temperature. *Remote Sensing of Environment*, *200*, 154–169. <https://doi.org/https://doi.org/10.1016/j.rse.2017.07.029>
- Daniilidis, A., Herber, R., & Vermaas, D. A. (2014). Upscale potential and financial feasibility of a reverse electro dialysis power plant. *Applied Energy*, *119*, 257–265. <https://doi.org/10.1016/J.APENERGY.2013.12.066>
- De Angelis, P., Tuninetti, M., Bergamasco, L., Calianno, L., Asinari, P., Laio, F., & Fasano, M. (2021). Data-driven appraisal of renewable energy potentials for sustainable freshwater production in Africa. *Renewable and Sustainable Energy Reviews*, *149*. <https://doi.org/10.1016/J.RSER.2021.111414>
- Długolecki, P., Gambier, A., Nijmeijer, K., & Wessling, M. (2009). Practical potential of reverse electro dialysis as process for sustainable energy generation. *Environmental Science and Technology*, *43*(17), 6888–6894. https://doi.org/10.1021/ES9009635/ASSET/IMAGES/LARGE/ES-2009-009635_0004.JPEG
- Doorga, J. R. S., Hall, J. W., & Eyre, N. (2022). Geospatial multi-criteria analysis for identifying optimum wind and solar sites in Africa: Towards effective power sector decarbonization. *Renewable and Sustainable Energy Reviews*, *158*, 112107. <https://doi.org/https://doi.org/10.1016/j.rser.2022.112107>
- El Hacen Jed, M., Ihaddadene, R., Ihaddadene, N., Elhadji Sidi, C. Elb., & EL Bah, M. (2020). Performance analysis of 954,809 kWp PV array of Sheikh Zayed solar power plant (Nouakchott, Mauritania). *Renewable Energy Focus*, *32*, 45–54. <https://doi.org/10.1016/J.REF.2019.11.002>
- Emdadi, A., Gikas, P., Farazaki, M., & Emami, Y. (2016). Salinity gradient energy potential at the hyper saline Urmia Lake - ZarrinehRud River system in Iran. *Renewable Energy*, *86*, 154–162. <https://doi.org/10.1016/j.renene.2015.08.015>
- FAO. (2020). FAO. 2020. WaPOR database methodology: Version 2 release, April 2020. Rome. In *WaPOR database methodology* (Issue April). <https://doi.org/10.4060/ca9894en>
- Gerbo, A., Suryabagavan, K. V., & Kumar Raghuvanshi, T. (2020). GIS-based approach for modeling grid-connected solar power potential sites: a case study of East Shewa Zone, Ethiopia.

<https://doi.org/10.1080/24749508.2020.1809059>

Goal 7 | Department of Economic and Social Affairs. (2022). <https://sdgs.un.org/goals/goal7>

- Goffetti, G., Montini, M., Volpe, F., Gigliotti, M., Pulselli, F. M., Sannino, G., & Marchettini, N. (2018). Disaggregating the SWOT Analysis of Marine Renewable Energies. *Frontiers in Energy Research*, 6. <https://doi.org/10.3389/fenrg.2018.00138>
- Haddout, S., & Priya, K. L. (2020). Impacts of flushing time and intrusion length on electricity production from salinity gradient energy (SGE) in the estuaries. *International Journal of River Basin Management*, 0(0), 1–3. <https://doi.org/10.1080/15715124.2020.1750422>
- Heiba, B., Yahya, A. M., Taha, M. Q., Khezam, N., & Mahmoud, A. K. (2021). Performance analysis of 30 MW wind power plant in an operation mode in Nouakchott, Mauritania. *International Journal of Power Electronics and Drive Systems (IJPEDS)*, 12(1), 532–541. <https://doi.org/10.11591/IJPEDS.V12.I1.PP532-541>
- Helfer, F., & Lemckert, C. (2015). The power of salinity gradients: An Australian example. *Renewable and Sustainable Energy Reviews*, 50, 1–16. <https://doi.org/10.1016/j.rser.2015.04.188>
- Helfer, F., Lemckert, C., & Anissimov, Y. G. (2014). Osmotic power with Pressure Retarded Osmosis: Theory, performance and trends – A review. *Journal of Membrane Science*, 453, 337–358. <https://doi.org/10.1016/J.MEMSCI.2013.10.053>
- Huffman, G. J., Stocker, E. F., Bolvin, D. T., Nelkin, E. J., & Jackson, T. (2019). *GPM IMERG Final Precipitation L3 1 day 0.1 degree x 0.1 degree V06*. <https://doi.org/10.5067/GPM/IMERGDF/DAY/06>
- IEA. (2019). *Africa Energy Outlook 2019 - Analysis and key findings. A report by the International Energy Agency*. 288. www.iea.org/africa2019
- Jahromi, A. S., Lari, K., Morsali, A., Bidokhti, A. A., & Fard, M. J. S. (2015). e. *Indian Journal of Geo-Marine Sciences*, 44(12), 1867–1873.
- Jia, Z., Wang, B., Song, S., & Fan, Y. (2014a). Blue energy: Current technologies for sustainable power generation from water salinity gradient. *Renewable and Sustainable Energy Reviews*, 31, 91–100. <https://doi.org/10.1016/j.rser.2013.11.049>
- Jia, Z., Wang, B., Song, S., & Fan, Y. (2014b). Blue energy: Current technologies for sustainable power generation from water salinity gradient. *Renewable and Sustainable Energy Reviews*, 31, 91–100. <https://doi.org/10.1016/J.RSER.2013.11.049>
- Kang, S., Li, J., Wang, Z., Zhang, C., & Kong, X. (2022). Salinity gradient energy capture for power production by reverse electrodialysis experiment in thermal desalination plants. *Journal of Power Sources*, 519, 230806. <https://doi.org/10.1016/j.jpowsour.2021.230806>
- Kassem, Y., Çamur, H., & Abugharara, M. A. (2019). Assessment of Wind Energy Potential for Selecting Small-Scale Wind Turbines in Low Wind Locations in Libya: A Comparative Study. *International Journal of Engineering Research and Technology*, 12(6), 820–836. <http://www.irphouse.com>
- Kempener, R., & Neumann, F. (2014). Salinity Gradient Energy Conversion. *IRENA Ocean Energy Technology Brief 2, June*. <https://www.irena.org/publications/2014/Jun/Salinity-gradient>
- Khodadadian Elikaiy, S., Lari, K., Torabi Azad, M., Sabetahd Jahromi, A., & Mohseni Arasteh, A. (2021). Investigation and evaluation of salinity gradient power in Arvand River estuary using pressure retarded osmosis (PRO) method. *International Journal of Environmental Science and Technology*, 18(2), 463–470. <https://doi.org/10.1007/S13762-020-02993-6/TABLES/4>
- Kingsbury, R. S., Liu, F., Zhu, S., Boggs, C., Armstrong, M. D., Call, D. F., & Coronell, O. (2017). Impact of natural organic matter and inorganic solutes on energy recovery from five real salinity gradients using

- reverse electrodialysis. *Journal of Membrane Science*, 541, 621–632. <https://doi.org/10.1016/J.MEMSCI.2017.07.038>
- Kuleszo, J., Kroeze, C., Post, J., & Fekete, B. M. (2010). The potential of blue energy for reducing emissions of CO₂ and non-CO₂ greenhouse gases. *Journal of Integrative Environmental Sciences*, 7(sup1), 89–96. <https://doi.org/10.1080/19438151003680850>
- Lewis, A., Estefen, S., Huckerby, J., Musial, W., Pontes, T., & Torres-Martinez, J. (2011). Ocean energy. In Y. Sokona, K. Seyboth, P. Matschoss, S. Kadner, T. Zwickel, P. Eickemeier, G. Hansen, S. Schlomer, & C. von Stechow (Eds.), *Ocean Energy* (pp. 1–262). Cambridge University Press, Cambridge, United Kingdom and New York, NY, USA. <https://doi.org/10.1007/978-3-540-77932-2>
- Lin, S., Straub, A. P., & Elimelech, M. (2014). Thermodynamic limits of extractable energy by pressure retarded osmosis. *Energy & Environmental Science*, 7(8), 2706–2714. <https://doi.org/10.1039/C4EE01020E>
- Loeb, S. (2001). One hundred and thirty benign and renewable megawatts from Great Salt Lake? The possibilities of hydroelectric power by pressure-retarded osmosis. *Desalination*, 141(1), 85–91. [https://doi.org/10.1016/S0011-9164\(01\)00392-7](https://doi.org/10.1016/S0011-9164(01)00392-7)
- Loeb, S. (2002). Large-scale power production by pressure-retarded osmosis, using river water and sea water passing through spiral modules. *Desalination*, 143(2), 115–122. [https://doi.org/10.1016/S0011-9164\(02\)00233-3](https://doi.org/10.1016/S0011-9164(02)00233-3)
- Loeb, S., & Norman, R. S. (1975). Osmotic Power Plants. *Science*, 189(4203), 654 LP – 655. <https://doi.org/10.1126/science.189.4203.654>
- Logan, B. E., & Elimelech, M. (2012). Membrane-based processes for sustainable power generation using water. *Nature* 2012 488:7411, 488(7411), 313–319. <https://doi.org/10.1038/NATURE11477>
- Maisonneuve, J., Pillay, P., & Laflamme, C. B. (2015). Osmotic power potential in remote regions of Quebec. *Renewable Energy*, 81, 62–70. <https://doi.org/10.1016/J.RENENE.2015.03.015>
- Maka, A. O. M., Salem, S., & Mehmood, M. (2021). Solar photovoltaic (PV) applications in Libya: Challenges, potential, opportunities and future perspectives. *Cleaner Engineering and Technology*, 5, 100267. <https://doi.org/10.1016/J.CLET.2021.100267>
- Marin-Coria, E., Silva, R., Enriquez, C., Martínez, M. L., & Mendoza, E. (2021). *Salinity Gradient Energy Pilot Plant*. 1–24.
- Mendoza, E., Lithgow, D., Flores, P., Felix, A., Simas, T., & Silva, R. (2019). A framework to evaluate the environmental impact of OCEAN energy devices. *Renewable and Sustainable Energy Reviews*, 112, 440–449. <https://doi.org/https://doi.org/10.1016/j.rser.2019.05.060>
- Olabi, A. G., & Abdelkareem, M. A. (2022). Renewable energy and climate change. *Renewable and Sustainable Energy Reviews*, 158, 112111. <https://doi.org/https://doi.org/10.1016/j.rser.2022.112111>
- Olmedo, E., González-Haro, C., Hoareau, N., Umbert, M., González-Gambau, V., Martínez, J., Gabarró, C., & Turiel, A. (2021). Nine years of SMOS sea surface salinity global maps at the Barcelona Expert Center. *Earth System Science Data*, 13(2), 857–888. <https://doi.org/10.5194/essd-13-857-2021>
- Pattle, R. E. (1954). Production of Electric Power by mixing Fresh and Salt Water in the Hydroelectric Pile. *Nature* 1954 174:4431, 174(4431), 660–660. <https://doi.org/10.1038/174660a0>
- Population of Africa (2022) - Worldometer*. (2022). <https://www.worldometers.info/world-population/africa-population/>
- Post, J. W., Veerman, J., Hamelers, H. V. M., Euverink, G. J. W., Metz, S. J., Nymeiijer, K., & Buisman, C. J. N. (2007). Salinity-gradient power: Evaluation of pressure-retarded osmosis and reverse electrodialysis. *Journal of Membrane Science*, 288(1–2), 218–230. <https://doi.org/10.1016/J.MEMSCI.2006.11.018>

- R. Pattle. (1954). NATU RE October 2, 1954. *Nature*, 174(1953), <https://doi.org/10.1038/174660a0>.
- Reuter, H. I., Nelson, A., & Jarvis, A. (2007). An evaluation of void-filling interpolation methods for SRTM data. *International Journal of Geographical Information Science*, 21(9), 983–1008. <https://doi.org/10.1080/13658810601169899>
- Reyes-Mendoza, O., Alvarez-Silva, O., Chiappa-Carrara, X., & Enriquez, C. (2020). Variability of the thermohaline structure of a coastal hypersaline lagoon and the implications for salinity gradient energy harvesting. *Sustainable Energy Technologies and Assessments*, 38(August 2019), 100645. <https://doi.org/10.1016/j.seta.2020.100645>
- Saleh, F., Ramaswamy, V., Georgas, N., Blumberg, A. F., & Pullen, J. (2018). Inter-comparison between retrospective ensemble streamflow forecasts using meteorological inputs from ECMWF and NOAA/ESRL in the Hudson River sub-basins during Hurricane Irene (2011). *Hydrology Research*, 50(1), 166–186. <https://doi.org/10.2166/nh.2018.182>
- Schaetzle, O., & Buisman, C. J. N. (2015). Salinity Gradient Energy: Current State and New Trends. *Www.Engineering.Org.Cn News & Focus Engineering*, 1(2), 164–166. <https://doi.org/10.15302/J-ENG-2015046>
- Sharma, M., Das, P. P., Chakraborty, A., & Purkait, M. K. (2022). Clean energy from salinity gradients using pressure retarded osmosis and reverse electrodialysis: A review. *Sustainable Energy Technologies and Assessments*, 49, 101687. <https://doi.org/10.1016/J.SETA.2021.101687>
- Stenzel, P., & Wagner, H. (2010). Osmotic power plants: Potential analysis and site criteria. *3rd International Conference on Ocean Energy*, ..., January, 1–5. <http://scholar.google.com/scholar?hl=en&btnG=Search&q=intitle:Osmotic+power+plants++Potential+analysis+and+site+criteria#0>
- Thorsen, T., & Holt, T. (2009). The potential for power production from salinity gradients by pressure retarded osmosis. *Journal of Membrane Science*, 335(1–2), 103–110. <https://doi.org/10.1016/j.memsci.2009.03.003>
- Turek, M., Bandura, B., & Dydo, P. (2008). Power production from coal-mine brine utilizing reversed electrodialysis. *Desalination*, 221(1–3), 462–466. <https://doi.org/10.1016/J.DESAL.2007.01.106>
- Ulloa, J., Ballari, D., Campozano, L., & Samaniego, E. (2017). Two-Step Downscaling of Trmm 3b43 V7 Precipitation in Contrasting Climatic Regions With Sparse Monitoring: The Case of Ecuador in Tropical South America. *Remote Sensing*, 9(7). <https://doi.org/10.3390/rs9070758>
- Veerman, J., Saakes, M., Metz, S. J., & Harmsen, G. J. (2010). Electrical power from sea and river water by reverse electrodialysis: A first step from the laboratory to a real power plant. *Environmental Science and Technology*, 44(23), 9207–9212. https://doi.org/10.1021/ES1009345/ASSET/IMAGES/LARGE/ES-2010-009345_0003.JPEG
- Vermaas, D. A., Guler, E., Saakes, M., & Nijmeijer, K. (2012). Theoretical power density from salinity gradients using reverse electrodialysis. *Energy Procedia*, 20, 170–184. <https://doi.org/10.1016/J.EGYPRO.2012.03.018>
- Water Scarcity | Threats | WWF*. (2022). <https://www.worldwildlife.org/threats/water-scarcity>
- Wick, G. L. (1978). Power from salinity gradients. *Energy*, 3(1), 95–100. [https://doi.org/10.1016/0360-5442\(78\)90059-2](https://doi.org/10.1016/0360-5442(78)90059-2)
- Yin Yip, N., Brogioli, D., M Hamelers, H. V., & Nijmeijer, K. (2016). *Salinity Gradients for Sustainable Energy: Primer, Progress, and Prospects*. <https://doi.org/10.1021/acs.est.6b03448>
- Yip, N. Y., & Elimelech, M. (2014). Comparison of energy efficiency and power density in pressure retarded osmosis and reverse electrodialysis. *Environmental Science and Technology*, 48(18), 11002–11012. https://doi.org/10.1021/ES5029316/SUPPL_FILE/ES5029316_SI_001.PDF

- Yip, N. Y., Tiraferri, A., Phillip, W. A., Schiffman, J. D., Hoover, L. A., Kim, Y. C., & Elimelech, M. (2011). Thin-film composite pressure retarded osmosis membranes for sustainable power generation from salinity gradients. *Environmental Science and Technology*, 45(10), 4360–4369. https://doi.org/10.1021/ES104325Z/SUPPL_FILE/ES104325Z_SI_001.PDF
- Zachopoulos, K., Kokkos, N., Elmasides, C., & Sylaios, G. (2022). Coupling Hydrodynamic and Energy Production Models for Salinity Gradient Energy Assessment in a Salt-Wedge Estuary (Strymon River, Northern Greece). *Energies*, 15(9). <https://doi.org/10.3390/en15092970>
- Zanaga, D., Van De Kerchove, R., De Keersmaecker, W., Souverijns, N., Brockmann, C., Quast, R., Wevers, J., Grosu, A., Paccini, A., Vergnaud, S., Cartus, O., Santoro, M., Fritz, S., Georgieva, I., Lesiv, M., Carter, S., Herold, M., Li, L., Tsendbazar, N.-E., ... Arino, O. (2021). *ESA WorldCover 10 m 2020 v100*. <https://doi.org/10.5281/ZENODO.5571936>
- Zougrana, A., Türk, O. K., & Çakmakci, M. (2020). Energy coverage of ataköy-ambarlı municipal wastewater treatment plants by salinity gradient power. *Journal of Water Process Engineering*, 38. <https://doi.org/10.1016/J.JWPE.2020.101552>

10. Appendix

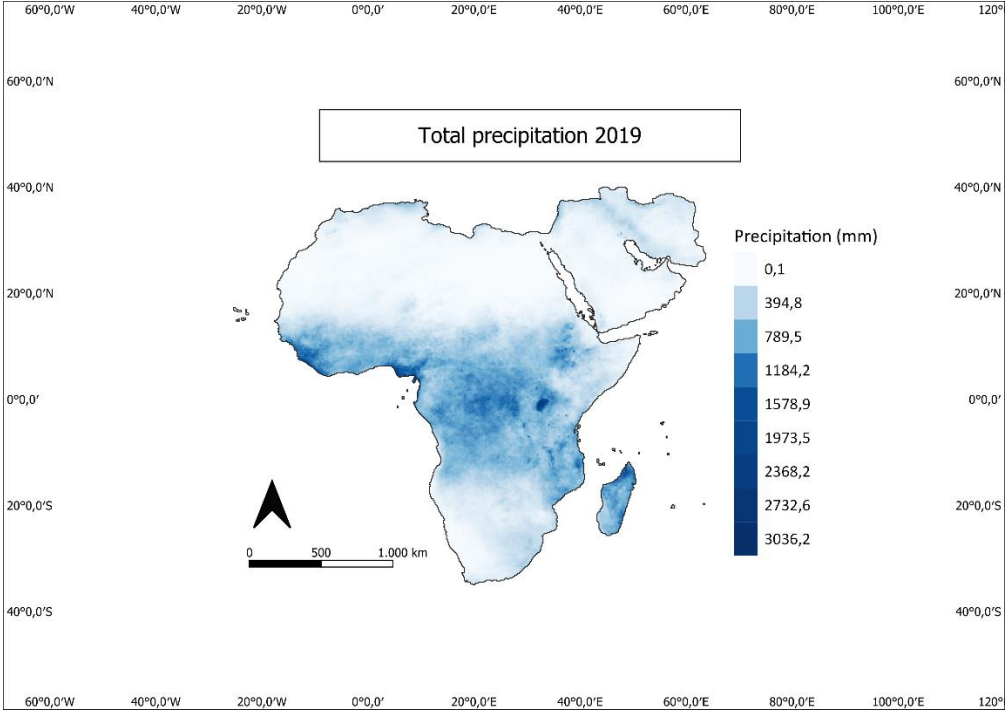


Figure 16 Total precipitation (mm) Africa -2019

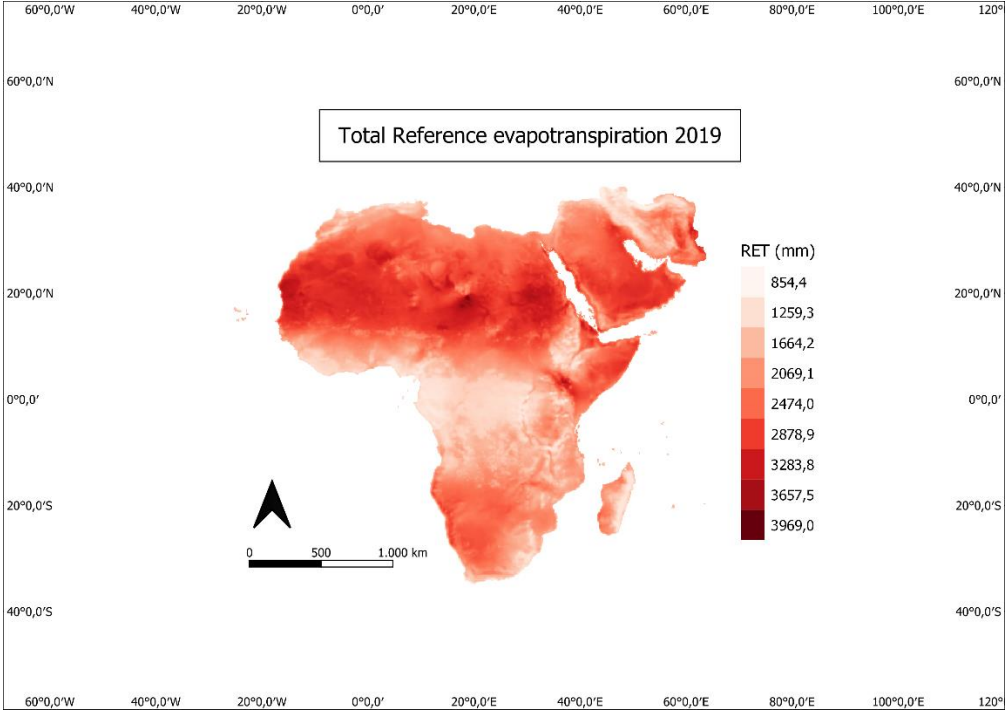


Figure 17 Total Reference evapotranspiration in Africa(mm)-2019

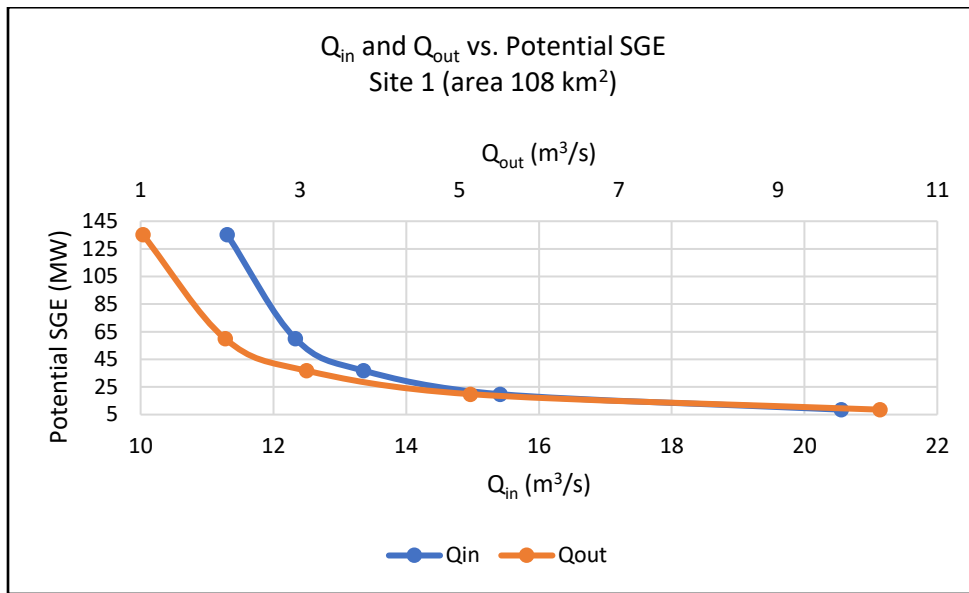


Figure 18: Q_{in} and Q_{out} vs. potential SGE for area of 108 km² in site 1

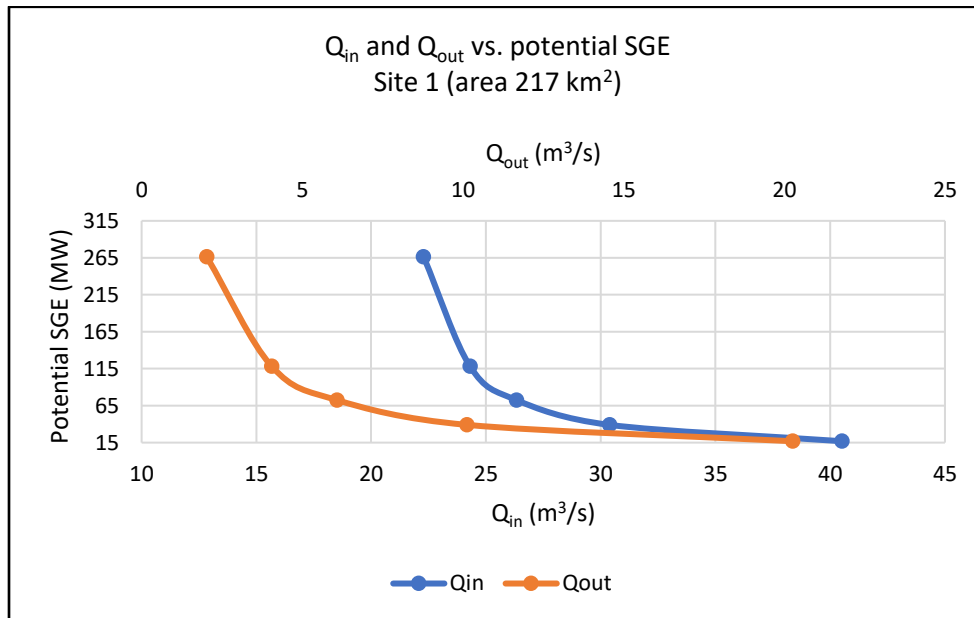


Figure 19 : Q_{in} and Q_{out} vs. potential SGE for area of 217 km² in site 1

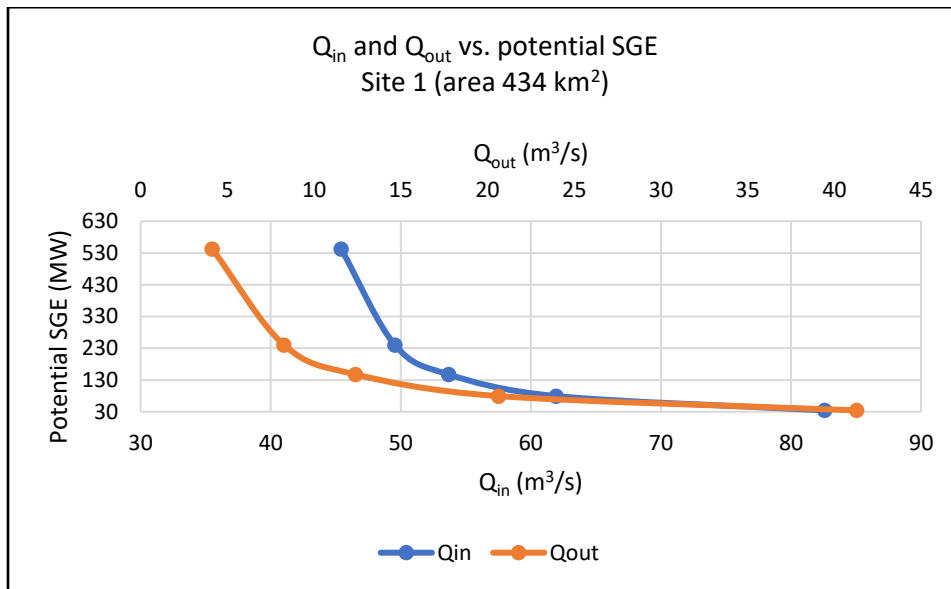


Figure 20: Q_{in} and Q_{out} vs. potential SGE for area of 434 km² in site 1

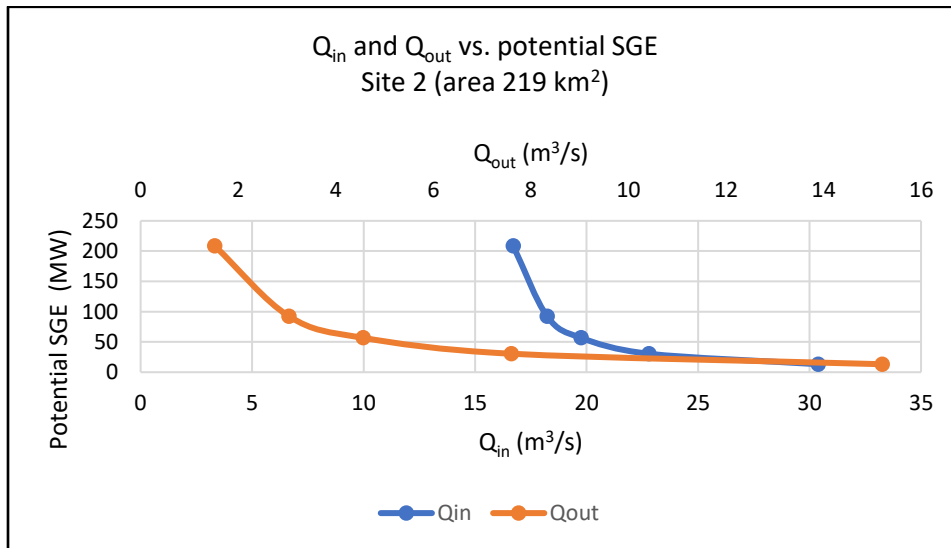


Figure 21: Q_{in} and Q_{out} vs. potential SGE for area of 219 km² in site 2